Ⅳ. 研究成果の刊行物・別刷

Proximal Promoter of the Cytochrome P450 Oxidoreductase Gene: Identification of Microdeletions Involving the Untranslated Exon 1 and Critical Function of the SP1 Binding Sites

Shun Soneda,* Takashi Yazawa,* Maki Fukami,* Masanori Adachi, Michiyo Mizota, Kenji Fujieda, Kaoru Miyamoto, and Tsutomu Ogata

Department of Molecular Endocrinology (S.S., M.F., T.O.), National Research Institute for Child Health and Development, Tokyo 157-8535, Japan; Department of Pediatrics (S.S.), St. Marianna University School of Medicine, Kawasaki 216-8511, Japan; Department of Biochemistry, Faculty of Medical Sciences (T.Y., K.M.), University of Fukui, Fukui 910-1193, Japan; Division of Endocrinology and Metabolism (M.A.), Kanagawa Children's Medical Center, Yokohama 232-8555, Japan; Department of Pediatrics (M.M.), Kagoshima University School of Medicine, Kagoshima 890-8520, Japan; Department of Pediatrics (K.F.), Asahikawa Medical Collage, Asahikawa 078-8510, Japan; and Department of Pediatrics (T.O.), Hamamatsu University School of Medicine, Hamamatsu 431-3192, Japan

Context: *POR* (cytochrome P450 oxidoreductase) is a ubiquitously expressed gene encoding an electron donor to all microsomal P450 enzymes and several non-P450 enzymes. *POR* mutations cause an autosomal recessive disorder characterized by skeletal dysplasia, adrenal dysfunction, and disorders of sex development. Although recent studies have indicated the presence of a CpG-rich region characteristic of housekeeping genes around the untranslated exon 1 (exon 1U) and a tropic effect of thyroid hormone on *POR* expression via thyroid hormone receptor-β, detailed regulatory mechanisms for the *POR* expression remain to be clarified.

Objective: Our objective was to report a pivotal element of the proximal promoter of *POR*.

Results: We first studied three patients (cases 1–3) with POR deficiency due to compound heterozygosity with an p.R457H mutation and transcription failure of an apparently normal allele, by oligoarray comparative genomic hybridization and serial direct sequencing of the deletion fusion points. Consequently, a 2,487-bp microdeletion involving exon 1U was identified in case 1 and an identical 49,604-bp deletion involving exon 1U and exon 1 was found in cases 2 and 3. We next analyzed the 2,487-bp region commonly deleted in cases 1–3 by *in silico* analysis, DNA binding analysis, luciferase assays, and methylation analysis. The results showed a critical function of the evolutionally conserved SP1 binding sites just upstream of exon 1U, especially the binding site at the position −26/−17, in the transcription of *POR*.

Conclusions: The results suggest that the SP1 binding sites constitute an essential element of the *POR* proximal promoter. **(*J Clin Endocrinol Metab* 96: E1881–E1887, 2011)**

Cytochrome P450 (CYP) oxidoreductase (POR) deficiency (PORD) is a rare autosomal recessive disorder caused by mutations in the gene encoding a flavoprotein that functions as an electron donor to all microsomal P450 enzymes and several non-P450 enzymes (1–3). Salient clinical features of PORD include skeletal dysplasia referred to as Antley-Bixler syndrome, adrenal dysfunction, 46,XY and 46,XX disorders of sex development (DSD), and maternal virilization during pregnancy (1–4). Such features are primarily explained by impaired activities of POR-

ISSN Print 0021-972X ISSN Online 1945-7197
Printed in U.S.A.

doi: 10.1210/jc.2011-1337 Received April 25, 2011. Accepted August 18, 2011.
First Published Online September 7, 2011

* S.S., T.Y., and M.F. contributed equally to this work.

Abbreviations: CGH, Comparative genomic hybridization; CYP, cytochrome P450; DSD, disorders of sex development; exon 1U, untranslated exon 1; HEK, human embryonic kidney; POR, CYP oxidoreductase; PORD, POR deficiency; SL2, Schneider line 2.

dependent CYP51A1 and squalene epoxidase involved in cholesterologenesis and CYP17A1, CYP21A2, and CYP19A1 involved in steroidogenesis (1–4). Anorectal and urinary anomalies are also occasionally observed in PORD, probably due to decreased activity of CYP26 relevant to retinoic acid metabolism (5). The complete absence of POR activity is assumed to be lethal (4), and consistent with this, all the patients identified to date have at least one missense mutation that is likely to preserve some residual activity (1, 2, 6, 7). In addition, heterozygosity with one apparently normal allele has been reported in approximately 12% of PORD patients (4).

The *POR/Por* gene is transcribed ubiquitously with more or less variable expression levels among different tissues (8, 9). Consistent with the ubiquitous expression pattern, rat *Por* is known to be associated with a CpG-rich region (CpG islands) (9) characteristic of housekeeping genes (10). Similarly, human *POR* consists of a single untranslated exon 1 (exon 1U) and coding exons 1–15, and the region around exon 1U harbors a CpG-rich region (11). In addition, the SP1 binding sites as a potential proximal promoter element reside in the CpG-rich region of rat *Por* (9), whereas they have not yet been reported in the CpG-rich region of human *POR*. Furthermore, Tee *et al.* (12) have recently studied the approximately 300-bp proximal promoter region just upstream of exon 1U of human *POR*, showing that thyroid hormone exerts a major trophic effect on *POR* expression primarily via thyroid hormone receptor-β, with thyroid hormone receptor-α, estrogen receptor-α, Smad3, and Smad4 exerting lesser modulatory effects. However, the detailed regulatory mechanisms for the transcription of human *POR* remain to be clarified.

Here, we report two types of microdeletions, one involving exon 1U alone and the other involving exon 1U and exon 1, in patients with PORD and suggest a pivotal role of the SP1 binding sites in the transcriptional regulation of *POR*. The results, in conjunction with the previous data (12), provide significant progress in the clarification of the regulatory machinery for the expression of *POR*.

Patients and Methods

Patients

We examined three nonconsanguineous patients (case 1 with 46,XY and cases 2 and 3 with 46,XX) reported in our previous paper describing 35 patients with PORD (7); cases 1, 2, and 3 in this report correspond to cases 18, 26, and 27 in the previous paper, respectively. Cases 1–3 manifested Antley-Bixler syndrome-compatible skeletal features, adrenal dysfunction with

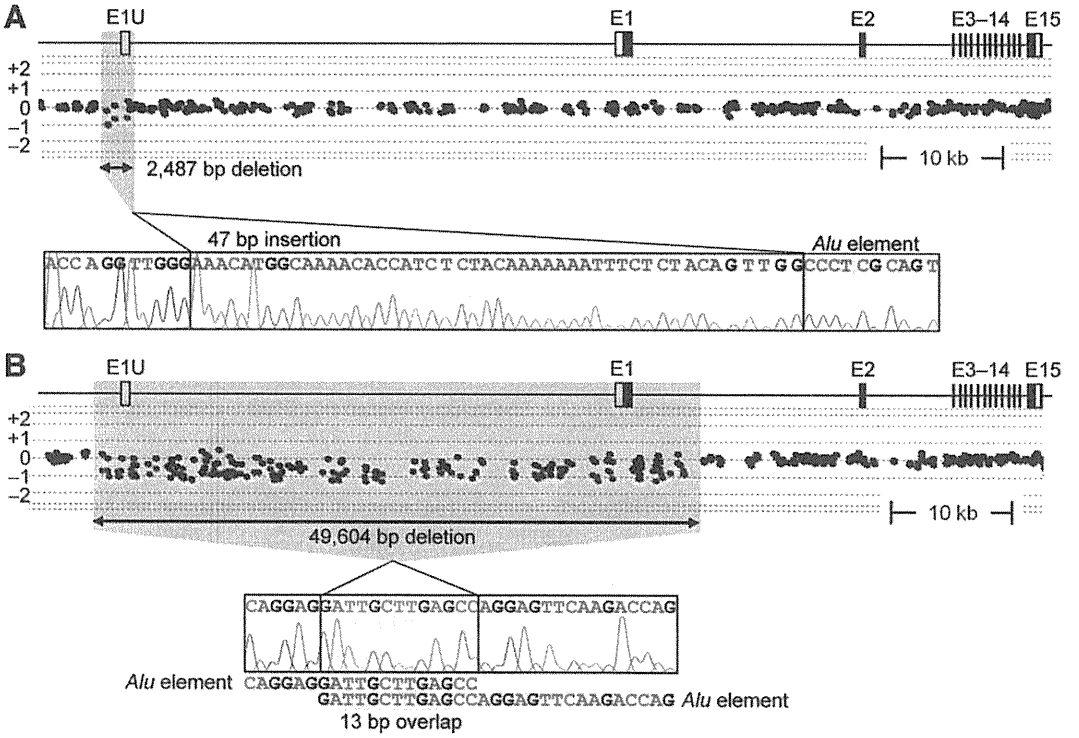

FIG. 1. Identification and characterization of the microdeletions in case 1 (panel A) and cases 2 and 3 (panel B) by CGH analysis and direct sequencing of the deletion junctions. The position of *POR* exons (E1U–E15) is shown on the CGH findings; the *black and white boxes* denote the coding regions and the untranslated regions, respectively. In the CGH results, the *black and green dots* denote signals indicative of the normal and the decreased (<−0.5) copy numbers, respectively. In the direct sequencing findings, the 47-bp segment inserted into the fusion point in case 1 is *highlighted* with *light yellow*, and the 13-bp overlapping sequence at the fusion point in cases 2 and 3 is *highlighted* with *light blue*. The *Alu* elements are indicated with *light blue bars*.

drastically compromised cortisol response to ACTH stimulation, and DSD (bilateral cryptorchidism in case 1, partial labial fusion in case 2, and mild clitoromegaly in case 3). Cases 2 and 3 also experienced adrenal crisis, whereas maternal virilization during pregnancy was not identified in cases 1–3. In addition, case 2 had right vesicoureteral reflux, and case 3 manifested imperforated anus. In cases 1–3, direct sequencing for leukocyte genomic DNA indicated apparent heterozygosity for the Japanese founder mutation p.R457H, and that for leukocyte cDNA demonstrated transcription failure of an apparently normal allele (7). Thus, although cases 1–3 were found to have compound heterozygosity for p.R457H and transcription failure, the cause of transcription failure remained to be clarified.

Primer and probe

The primers and probes used in the present study are shown in Supplemental Table 1 (published on The Endocrine Society's Journals Online web site at http://endo.endojournals.org).

Genome structure analysis

Oligoarray comparative genomic hybridization (CGH) was performed for leukocyte genomic DNA, using a custom-build oligo-microarray containing 39,169 probes for an approximately 8-Mb region around *POR* and 26,662 reference probes for a different genomic interval (2x105K format, design ID 022431) (Agilent Technologies, Palo Alto, CA). The procedure was as described in the manufacturer's instructions. To determine the deletion size and the junction structure, serial direct sequencing was performed for long PCR products obtained with primer pairs flanking the deleted region, and the obtained junction sequence was compared with the reference sequence at the NCBI Database (NT_007933.15). The presence or absence of repeat sequences around the breakpoints was examined with Repeatmasker (http://www.repeatmasker.org).

In silico analysis

In silico analysis was performed for CpG islands, evolutionally conserved sequences, and promoter-associated histone marks, using UCSC genome browser (http://genome.ucsc.edu/). Putative transcription factor binding sites were searched by TFSEARCH (http://mbs.cbrc.jp/research/db/TFSEARCH.html). In addition, because animal *Por* has been well studied in rats (9), conservation status of identified sites was examined using rat data. The transcription start site of *POR* exon 1U (+1) was determined on the basis of the *POR* cDNA sequence (NM_000941) obtained from the NCBI database.

Luciferase assays

A series of promoter-reporter constructs were generated by inserting PCR-amplified DNA fragments into PGL3-enhancer vector or pGL3-basic vector (Promega, Madison, WI). Deletion mutants were created by site-directed mutagenesis. Transient transfection was carried out using human embryonic kidney (HEK) 293 cells with endogenous SP families, because of their stable transfection efficiency and usefulness in *in vitro* functional studies for SP1 binding sites (13). HEK 293 cells were cultured in DMEM at 37 C, seeded in 12-well dishes, and transfected using Lipofectamine 2000 (Life Technologies, Carlsbad, CA) with 0.6 μg of the reporter plasmids. As an internal control for the transfection, 20 ng pRL-CMV vector (Promega) was used. In addition, transient transfection was also performed using *Drosophila* Schneider line 2 (SL2) cells (CRL-1963; American Type Culture Collection, Manassas, VA) that lack endogenous SP families. SL2 cells were grown in Schneider's medium at 25 C, seeded in six-well dishes, and transfected using calcium phosphate (14) with 1.0 μg of the reporter plasmid and a total of 50 ng of various combinations of the SP1 expression vector (pPAC-SP1) and an empty pPAC vector, as well as 50 ng of the SP3 expression vector (pPAC-SP3). As an internal control for the transfection, 50 ng pPAC-β-galactosidase vector was used. For both experiments using HEK 293 cells and SL2 cells, luciferase activities were determined at 48 h after the transfections.

Transfections were performed in triplicate within a single experiment, and the experiments were repeated three times. The results are expressed as mean ± SEM, and statistical significance was examined by the *t* test. $P < 0.05$ was considered significant.

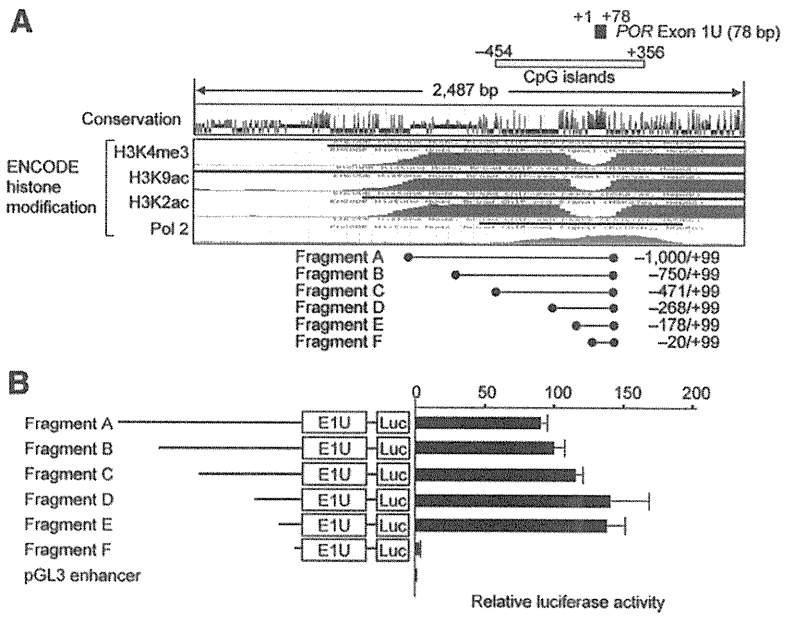

FIG. 2. Localization of the promoter region to a 178-bp segment just upstream of exon 1U. Panel A, *In silico* analysis in search of the promoter-compatible sequences. The transcription start site of *POR* exon 1U (+1) is based on the *POR* cDNA sequence at the NCBI database (NM_000941). The CpG-rich region spans from −454 to +356 bp. The ENCODE histone modification analysis indicates the presence of a highly conserved promoter-compatible sequence just upstream of exon 1U. The fragments A–F denote the DNA sequences used for the luciferase assays. Panel B, Luciferase reporter assays using the fragments A–F. The results are expressed as fold-change of the target vectors over the empty pGL3 enhancer vector (mean ± SEM). Transfections were performed in triplicate within a single experiment, and the experiments were repeated three times. Although the increase in the relative luciferase activity is significant for fragment A (92.6 ± 5.2, $P = 0.0006$), fragment B (101.6 ± 5.8, $P = 0.0006$), fragment C (106.0 ± 5.5, $P = 0.0004$), fragment D (137.7 ± 29.0, $P = 0.0009$), and fragment E (131.3 ± 13.4, $P = 0.0006$), it is not significant for fragment F (2.6 ± 1.1, $P = 0.25$).

DNA binding analysis

EMSA was performed as described previously (15). In brief, 10 μg of nuclear extracts of HEK 293 cells were incubated with ^{32}P-labeled oligonucleotides and unlabeled polydeoxyinosinic-deoxycytidylic acids and subjected to polyacrylamide gel electrophoresis (4%). For a competition experiment, a 200-fold molar excess of unlabeled competitor DNA was added. Supershift assay was performed by preincubating the nuclear extracts with anti-SP1 antisera (PEP2) and/or anti-SP3 antisera (D-20) (Santa Cruz Biotechnology, Santa Cruz, CA).

Methylation analysis

Bisulfite sequencing was performed for human leukocyte- and HEK 293-derived genomic DNA samples treated with the EZ DNA Methylation Kit (Zymo Research, Orange, CA) that converts all the cytosines except for methylated cytosines at the CpG dinucleotides into uracils and subsequently thymines. A 282-bp CpG-rich region containing SP1 binding sites just upstream of exon 1U was amplified with primer sets that hybridize to both methylated and unmethylated alleles because of absent CpG dinucleotides within the primer sequences. Subsequently, the PCR products were subcloned with the TOPO TA Cloning Kit (Life Technologies), and multiple clones were subjected to direct sequencing on the CEQ 8000 autosequencer (Beckman Coulter, Fullerton, CA).

Results

Identification and characterization of microdeletions in cases 1–3

Oligoarray CGH analysis indicated cryptic heterozygous deletions in cases 1–3 (Fig. 1). Furthermore, sequencing of the long PCR products harboring the fusion points revealed a 2,487-bp microdeletion (13,575,403–13,577,889 bp) encompassing exon 1U in case 1 and an identical 49,604-bp deletion (13,571,326–13,620,929 bp) involving exon 1U and exon 1 in cases 2 and 3. Thus, the 2,487-bp microdeletion on the noncoding upstream region was common to cases 1–3. The microdeletion in case

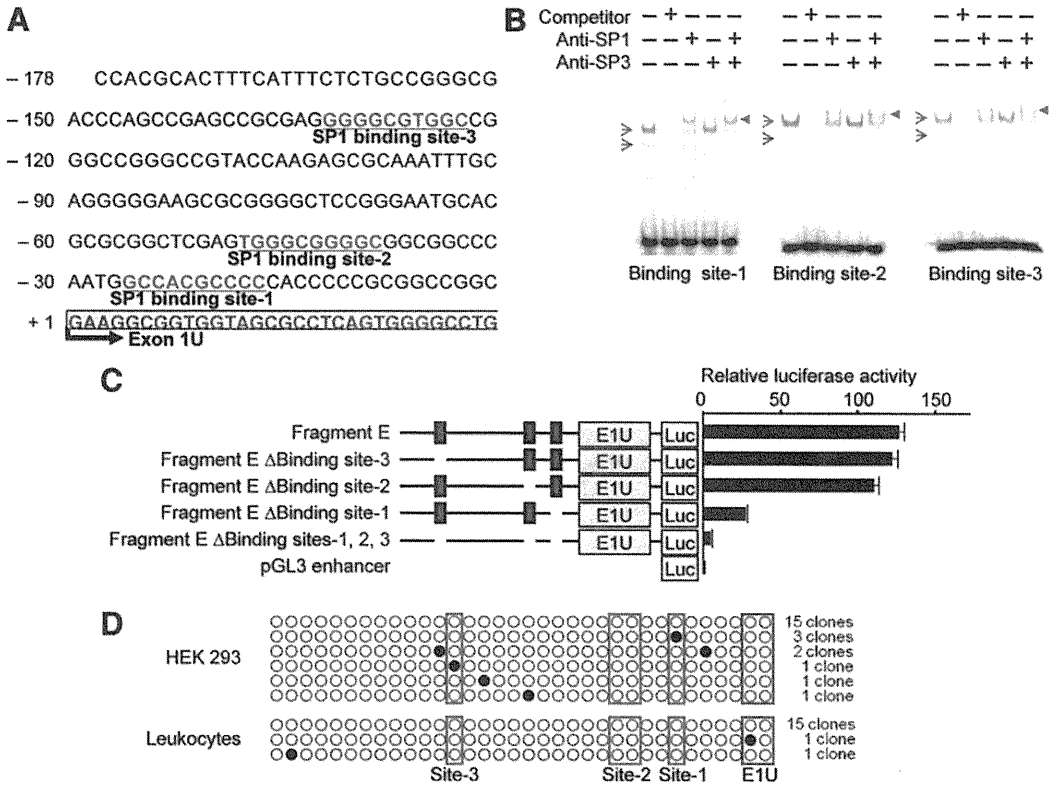

FIG. 3. Functional studies of the SP1 binding sites. Panel A, The three potential SP1 binding sites 1–3 at the position just upstream of exon 1U. The transcription start site of *POR* exon 1U (+1) is based on the *POR* cDNA sequence at the NCBI database (NM_000941). Panel B, EMSA showing positive bindings of SP1 and SP3 proteins to the SP1 binding sites 1–3. The *red arrows* indicate the strong bands derived from the SP1 protein binding to the probes containing the SP1 binding sites. These bands become weak, and supershifted bands (*red arrowheads*) are seen by adding anti-SP1. In addition, the *blue arrows* denote specific bands derived from the SP3 protein binding to the same probes. These bands become very weak by adding anti-SP3; the extremely faint supershifted bands are not visible in this figure. The band shift pattern is more obvious for SP1 protein than for SP3 protein. Panel C, Luciferase reporter assays using fragment E and its deletion mutants. The results are expressed as fold change of the target vectors over the empty pGL3 enhancer vector (mean ± SEM). Transfections were performed in triplicate within a single experiment, and the experiments were repeated three times. Although the relative luciferase activity is similar between Fragment E (121.8 ± 3.4) and ΔBinding site-3 (117.8 ± 3.1) ($P = 0.22$), it is significantly different between Fragment E and ΔBinding site-2 (105.7 ± 3.5) ($P = 0.015$), ΔBinding site-1 (25.8 ± 1.2) ($P = 0.0007$), and ΔBinding site-1, -2, and -3 (5.2 ± 0.5) ($P = 0.0004$). Panel D, Methylation analysis of the CpG-rich region. Each *circle* denotes a CpG island, and *filled* and *open circles* represent methylated and unmethylated cytosines, respectively. The CpG dinucleotides within the exon 1U are surrounded by *blue squares*, and those within the SP1 binding sites 1, 2, and 3 by *red squares*.

1 occurred between an *Alu* element and a nonrepeat sequence and was associated with an addition of a 47-bp segment of unknown origin, whereas that in cases 2 and 3 occurred between two *Alu* elements with an overlap of a 13-bp segment.

Critical function of the SP1 binding sites

In silico analysis for the noncoding 2,487-bp region showed an 810-bp long CpG-rich region involving exon 1U, an approximately 350-bp long evolutionally conserved sequence-rich region encompassing exon 1U, and an approximately 1.3-kb region with promoter-associated histone marks (Fig. 2A). The TATA box was not identified. Thus, relative luciferase activity was examined for fragments A–F with various lengths of the candidate promoter region, localizing a critical sequence for the *POR* promoter to a 178-bp segment defined by fragment E and fragment F (Fig. 2B).

The 178-bp segment was found to harbor three SP1 binding sites, *i.e.* site 1 at the position −26/−17, site 2 at the position −48/−39, and site 3 at the position −132/−123 (Fig. 3A). The three binding sites were well conserved in rats. EMSA indicated specific binding of SP1 and SP3 proteins to the three binding sites, with the band shift pattern being more obvious for SP1 protein than for SP3 protein (Fig. 3B). Deletion of the binding site 1 and the binding site 2 significantly reduced the relative luciferase activity (by ~80 and ~15%, respectively), although deletion of the binding site 3 had no significant effect on the relative luciferase activity; furthermore, loss of the binding sites 1–3 virtually abolished the relative luciferase activity (Fig. 3C). The 282-bp segment containing the three SP1 binding sites was almost completely unmethylated (Fig. 3D).

Furthermore, relative luciferase activity was examined for a 170-bp fragment (−120/+50) harboring the SP1 binding site 1 and the SP1 binding site 2, using SL2 cells devoid of endogenous SP families. Relative luciferase activity was clearly increased in a dose-dependent manner by adding the *SP1* expression vector but was barely elevated by adding the *SP3* expression vector (Fig. 4).

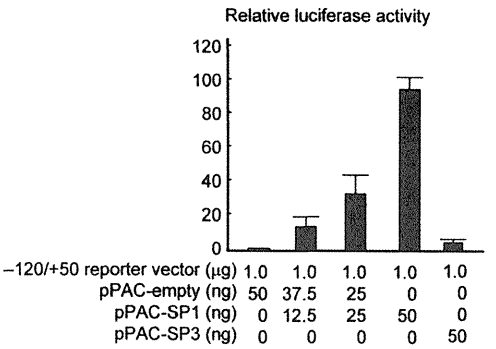

FIG. 4. Luciferase assays of a fragment containing the SP1 binding sites 1 and 2, using SL2 cells lacking endogenous SP families. The results are expressed as fold change of the target vectors over the empty pPAC vector (mean ± SEM). Transfections were performed in triplicate within a single experiment, and the experiments were repeated three times. The relative luciferase activity is significantly increased by adding the *SP1* expression vector of 12.5 ng (14.7 ± 4.4) ($P = 0.037$), 25.0 ng (31.8 ± 7.6) ($P = 0.035$), and 50 ng (95.8 ± 7.1) ($P = 0.0002$), although it is barely elevated by adding the *SP3* expression vector of 50 ng (5.2 ± 1.5) ($P = 0.054$).

Discussion

We identified two types of cryptic deletions, one involving exon 1U alone and the other encompassing exon 1U and exon 1, in three cases with PORD. The microdeletion in case 1 is explained by nonhomologous end joining that occurs between nonhomologous sequences and is frequently accompanied by an insertion of a short segment at the fusion point (16). The microdeletion in cases 2 and 3 is compatible with a repeat sequence mediated nonallelic intrachromosomal or interchromosomal recombination (16). Although cases 2 and 3 were apparently nonconsanguineous, it would not be unexpected that the same repeat-mediated genomic rearrangement took place in unrelated individuals. Notably, because the apparently normal allele in cases 1–3 was not transcribed (7), this implies that the 2,487-bp microdeletion common to cases 1–3 has affected the promoter function for *POR*. In this context, because approximately 12% of patients with PORD are known to be heterozygotes with one apparently normal *POR* allele (4), it might be possible that some, if not all, of them have similar microdeletions or other genetic aberrations affecting the *POR* transcription.

The present study revealed a pivotal role of the SP1 binding sites, especially the binding site 1, in the transcription of *POR*. This implies that the SP1 binding sites constitute an essential element of the *POR* proximal promoter. Indeed, SP1 binding sites as well as other noncore promoter elements are usually located in multiple copies within the proximal promoter region (~250 bp upstream of the transcription initiation site) of a ubiquitously expressed gene like *POR* (10). In this regard, several findings are noteworthy. First, the TATA box was apparently absent from the *POR* promoter region. This is compatible with the ubiquitous expression of *POR*, because the TATA box is usually identified in genes with a tissue-specific expression pattern (10). Second, the SP1 binding sites were highly conserved between the human and the rat. This finding, in conjunction with the previous data indicating absence of polymorphism for the three SP1 binding sites in 842 individuals (17), implies that the wild-type sequences of the SP1 binding sites are indispensable for the regulation of *POR* transcription. Third, the functional

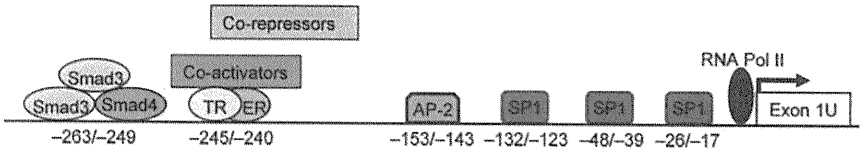

FIG. 5. Schematic representation indicating the binding sites for various factors in the proximal promoter region of *POR*. The diagram of the promoter upstream of −143 has been taken from Tee *et al.* (12). ER, Estrogen receptor; Pol II, polymerase II; TR, thyroid hormone receptor; AP-2, activator protein 2.

data using SL2 cells indicated a major role of SP1, rather than SP3, in the *POR* transcription. This is consistent with the notion that although both SP1 and SP3 can bind to the same cognate SP1 binding site, the DNA binding properties and regulatory functions are quite different between SP1 and SP3, depending on the promoter context and the cell type (18). Lastly, the SP1 binding sites were almost completely unmethylated. This argues for a transcriptionally active status of *POR*, because SP1 protein binding is known to be reduced when the CpG-rich region around the SP1 binding sites is methylated (19).

The proximal promoter region of *POR* has been studied previously (11, 12). Scott *et al.* (11) analyzed the 5′ region of *POR* coding exons by means of comparative genomics and characterized human *POR* exon 1U and its flanking sequences. Subsequently, Tee *et al.* (12) examined a 361-bp region around the transcription start site of exon 1U (−325/+36) using adrenal NCI-H295A and liver Hep-G2 cells and found a major trophic effect of thyroid hormone on *POR* expression primarily via thyroid hormone receptor-β as well as modulatory effects of thyroid hormone receptor-α, estrogen receptor-α, Smad3, and Smad4 on *POR* expression. The binding sites for these factors reside in a −263/−240 region upstream of the SP1 binding sites (Fig. 5). Furthermore, Tee *et al.* (12) screened functional alterations of polymorphisms within the 325-bp region, suggesting that the common −152C→A polymorphism may play a certain role in the genetic variation of steroid biosynthesis and drug metabolism. In this regard, whereas the −152C→A polymorphism resides on the AP-2 (activator protein 2) binding site, the functional difference of the polymorphism is obviously independent of the recruit of AP-2 (12). Thus, the underlying factors for the reduced activity of the −152A allele remain to be clarified.

Taken together, multiple regulatory elements have been identified in the proximal promoter region of *POR* (Fig. 5). Although the regulatory machinery has not yet been fully elucidated, we suggest that the presence of the SP1 binding sites has permitted the ubiquitous expression of *POR* and that the presence of other sites including thyroid hormone receptors is relevant to the variability in *POR* expression level among different tissues. In this regard, although the present study failed to identify the effects of the −263/−240 regulatory sequence identified by Tee *et al.* (12) (fragment D *vs.* fragment E in Fig. 2), this may be due to the difference in the cell type and/or in the promoter-luciferase construct used in the study by Tee *et al.* (+36) and in this study (+99). In addition, the hormonal effects on the *POR* transcription have not been examined in this study.

Finally, it would be useful to refer to clinical phenotypes of cases 1–3. In this context, we have previously compared clinical phenotype between Japanese PORD patients with homozygosity for the hypomorphic p.R457H mutation (group A) and those with compound heterozygosity for p.R457H and one apparently null mutation including nonsense and frameshift mutations (group B) and found that skeletal features are definitely more severe and adrenal dysfunction and 46,XY DSD are somewhat more severe in group B than in group A, whereas 46,XX DSD, maternal virilization during pregnancy, and anorectal and urinary anomalies are similarly identified in the two groups (5, 7). It is likely, therefore, that the residual POR activity reflected by the p.R457H dosage constitutes the underlying factor for clinical variability in some features but not in other features, probably due to the simplicity and complexity of POR-dependent metabolic pathways relevant to each phenotype. The clinical features of cases 1–3 are quite comparable to those of group B patients and, therefore, are consistent with transcription failure of one allele being a null mutation.

In summary, we identified microdeletions involving exon 1U and its upstream region in PORD patients, and revealed the critical function of the SP1 binding sites in the transcription of *POR*. Additional studies will permit to elucidate the regulatory machinery for *POR* expression.

Acknowledgments

We thank Dr. Timothy F. Osborne, University of California, Irvine, CA, and Dr. Guntram Suske, Philipps Universität, Marburg, Germany, for providing us with pPAC-β-galactosidase and pPAC-SP1/Sp3, respectively.

Address all correspondence and requests for reprints to: Dr. Maki Fukami, National Research Institute for Child Health and Development, Department of Endocrinology and Metabolism, 2-10-1 Ohkura, Setagaya, Tokyo 157-8535, Japan. E-mail: mfukami@nch.go.jp.

This work was supported by the Grant-in-Aid for Scientific Research on Innovative Areas (22132004) from the Ministry of Education, Culture, Sports, Science, and Technology (MEXT); by the Grant-in-Aid for Scientific Research (S) (22227002) from

the Japan Society for the Promotion of Science (JSPS); by the Grants for Research on Intractable Diseases (H22-098) and for Health Research on Children, Youth, and Families (H21-005) from the Ministry of Health, Labor and Welfare; by the Grant from Japan Foundation for Pediatric Research (10-001); and by the Grant of National Center for Child Health and Development (23A-1).

Disclosure Summary: The authors have nothing to declare.

References

1. **Flück CE, Tajima T, Pandey AV, Arlt W, Okuhara K, Verge CF, Jabs EW, Mendonça BB, Fujieda K, Miller WL** 2004 Mutant P450 oxidoreductase causes disordered steroidogenesis with and without Antley-Bixler syndrome. Nat Genet 36:228–230
2. **Arlt W, Walker EA, Draper N, Ivison HE, Ride JP, Hammer F, Chalder SM, Borucka-Mankiewicz M, Hauffa BP, Malunowicz EM, Stewart PM, Shackleton CH** 2004 Congenital adrenal hyperplasia caused by mutant P450 oxidoreductase and human androgen synthesis: analytical study. Lancet 363:2128–2135
3. **Miller WL** 2004 P450 oxidoreductase deficiency: a new disorder of steroidogenesis with multiple clinical manifestations. Trends Endocrinol Metab 15:311–315
4. **Scott RR, Miller WL** 2008 Genetic and clinical features of P450 oxidoreductase deficiency. Horm Res 69:266–275
5. **Fukami M, Nagai T, Mochizuki H, Muroya K, Yamada G, Takitani K, Ogata T** 2010 Anorectal and urinary anomalies and aberrant retinoic acid metabolism in cytochrome P450 oxidoreductase deficiency. Mol Genet Metab 100:269–273
6. **Huang N, Pandey AV, Agrawal V, Reardon W, Lapunzina PD, Mowat D, Jabs EW, Van Vliet G, Sack J, Flück CE, Miller WL** 2005 Diversity and function of mutations in P450 oxidoreductase in patients with Antley-Bixler syndrome and disordered steroidogenesis. Am J Hum Genet 76:729–749
7. **Fukami M, Nishimura G, Homma K, Nagai T, Hanaki K, Uematsu A, Ishii T, Numakura C, Sawada H, Nakacho M, Kowase T, Motomura K, Haruna H, Nakamura M, Ohishi A, Adachi M, Tajima T, Hasegawa Y, Hasegawa T, Horikawa R, Fujieda K, Ogata T** 2009 Cytochrome P450 oxidoreductase deficiency: identification and characterization of biallelic mutations and genotype-phenotype correlations in 35 Japanese patients. J Clin Endocrinol Metab 94: 1723–1731
8. **Shephard EA, Palmer CN, Segall HJ, Phillips IR** 1992 Quantification of cytochrome P450 reductase gene expression in human tissues. Arch Biochem Biophys 294:168–172
9. **O'Leary KA, Kasper CB** 2000 Molecular basis for cell-specific regulation of the NADPH-cytochrome P450 oxidoreductase gene. Arch Biochem Biophys 379:97–108
10. **Strachan T, Read AP** 2004 Human gene expression. In: Strachan T, Read AP, eds. Human molecular genetics. 3rd ed. New York: Garland Science; 275–313
11. **Scott RR, Gomes LG, Huang N, Van Vliet G, Miller WL** 2007 Apparent manifesting heterozygosity in P450 oxidoreductase deficiency and its effect on coexisting 21-hydroxylase deficiency. J Clin Endocrinol Metab 92:2318–2322
12. **Tee MK, Huang N, Damm I, Miller WL** 2011 Transcriptional regulation of the human P450 oxidoreductase gene: hormonal regulation and influence of promoter polymorphisms. Mol Endocrinol 25:715–731
13. **Blondet A, Gout J, Durand P, Bégeot M, Naville D** 2005 Expression of the human melanocortin-4 receptor gene is controlled by several members of the Sp transcription factor family. J Mol Endocrinol 34:317–329
14. **Di Nocera PP, Dawid IB** 1983 Transient expression of genes introduced into cultured cells of Drosophila. Proc Natl Acad Sci USA 80:7095–7098
15. **Yazawa T, Mizutani T, Yamada K, Kawata H, Sekiguchi T, Yoshino M, Kajitani T, Shou Z, Miyamoto K** 2003 Involvement of cyclic adenosine 5′-monophosphate response element-binding protein, steroidogenic factor 1, and Dax-1 in the regulation of gonadotropin-inducible ovarian transcription factor 1 gene expression by follicle-stimulating hormone in ovarian granulosa cells. Endocrinology 144:1920–1930
16. **Gu W, Zhang F, Lupski JR** 2008 Mechanisms for human genomic rearrangements. Pathogenetics 1:4
17. **Huang N, Agrawal V, Giacomini KM, Miller WL** 2008 Genetics of P450 oxidoreductase: Sequence variation in 842 individuals of four ethnicities and activities of 15 missense mutations. Proc Natl Acad Sci USA 105:1733–1738
18. **Li L, He S, Sun JM, Davie JR** 2004 Gene regulation by Sp1 and Sp3. Biochem Cell Biol 82:460–471
19. **Zhu WG, Srinivasan K, Dai Z, Duan W, Druhan LJ, Ding H, Yee L, Villalona-Calero MA, Plass C, Otterson GA** 2003 Methylation of adjacent CpG sites affects Sp1/Sp3 binding and activity in the p21(Cip1) promoter. Mol Cell Biol 23:4056–4065

Journal of Human Genetics (2011) 56, 91–93

www.nature.com/jhg

SHORT COMMUNICATION

Androgenetic/biparental mosaicism in a girl with Beckwith–Wiedemann syndrome-like and upd(14)pat-like phenotypes

Kazuki Yamazawa[1,5], Kazuhiko Nakabayashi[2], Kentaro Matsuoka[3], Keiko Masubara[1], Kenichiro Hata[2], Reiko Horikawa[4] and Tsutomu Ogata[1]

This report describes androgenetic/biparental mosaicism in a 4-year-old Japanese girl with Beckwith–Wiedemann syndrome (BWS)-like and paternal uniparental disomy 14 (upd(14)pat)-like phenotypes. We performed methylation analysis for 18 differentially methylated regions on various chromosomes, genome-wide microsatellite analysis for a total of 90 loci and expression analysis of *SNRPN* in leukocytes. Consequently, she was found to have an androgenetic 46,XX cell lineage and a normal 46,XX cell lineage, with the frequency of the androgenetic cells being roughly calculated as 91% in leukocytes, 70% in tongue tissues and 79% in tonsil tissues. It is likely that, after a normal fertilization between an ovum and a sperm, the paternally derived pronucleus alone, but not the maternally derived pronucleus, underwent a mitotic division, resulting both in the generation of the androgenetic cell lineage by endoreplication of one blastomere containing a paternally derived pronucleus and in the formation of the normal cell lineage by union of paternally and maternally derived pronuclei. It appears that the extent of overall (epi)genetic aberrations exceeded the threshold level for the development of BWS-like and upd(14)pat-like phenotypes, but not for the occurrence of other imprinting disorders or recessive Mendelian disorders.
Journal of Human Genetics (2011) **56,** 91–93; doi:10.1038/jhg.2010.142; published online 11 November 2010

Keywords: androgenesis; Beckwith–Wiedemann syndrome; mosaicism; upd(14)pat

INTRODUCTION

A pure androgenetic human with paternal uniparental disomy for all chromosomes is incompatible with life because of genomic imprinting.[1,2] However, a human with an androgenetic cell lineage could be viable in the presence of a normal cell lineage. Indeed, an androgenetic cell lineage has been identified in six liveborn individuals with variable phenotypes.[3–7] All the androgenetic cell lineages have a 46,XX karyotype, and this is consistent with the lethality of an androgenetic 46,YY cell lineage.

Here, we report on a girl with androgenetic/biparental mosaicism, and discuss the underlying factors for the phenotypic development.

CASE REPORT

This patient was conceived naturally to non-consanguineous and healthy parents. At 24 weeks gestation, the mother was referred to us because of threatened premature delivery. Ultrasound studies showed Beckwith–Wiedemann syndrome (BWS)-like features,[8] such as macroglossia, organomegaly and umbilical hernia, together with polyhydramnios and placentomegaly. The mother repeatedly received amnioreduction and tocolysis.

She was delivered by an emergency cesarean section because of preterm rupture of membranes at 34 weeks of gestation. Her birth weight was 3730 g (+4.8 s.d. for gestational age), and her length 45.6 cm (+0.7 s.d.). The placenta weighed 1040 g (+7.3 s.d.).[9] She was admitted to a neonatal intensive care unit due to asphyxia. Physical examination confirmed a BWS-like phenotype. Notably, chest roentgenograms delineated mild bell-shaped thorax characteristic of paternal uniparental disomy 14 (upd(14)pat),[10] although coat hanger appearance of the ribs indicative of upd(14)pat was absent (Supplementary Figure 1). She was placed on mechanical ventilation for 2 months, and received tracheostomy, glossectomy and tonsillectomy in her infancy, due to upper airway obstruction. She also had several clinical features occasionally reported in BWS[8] (Supplementary Table 1). Her karyotype was 46,XX in all the 50 lymphocytes analyzed. On the last examination at 4 years of age, she showed postnatal growth failure and severe developmental retardation.

[1]Department of Molecular Endocrinology, National Research Institute for Child Health and Development, Tokyo, Japan; [2]Department of Maternal-Fetal Biology, National Research Institute for Child Health and Development, Tokyo, Japan; [3]Division of Pathology, National Medical Center for Children and Mothers, Tokyo, Japan and [4]Division of Endocrinology and Metabolism, National Medical Center for Children and Mothers, Tokyo, Japan
[5]Current address: Department of Physiology, Development & Neuroscience, University of Cambridge, Cambridge, UK.
Correspondence: Dr T Ogata, Department of Molecular Endocrinology, National Research Institute for Child Health and Development, 2-10-1 Ohkura, Setagaya, Tokyo 157-8535, Japan.
E-mail: tomogata@nch.go.jp
Received 9 September 2010; revised 18 October 2010; accepted 22 October 2010; published online 11 November 2010

MOLECULAR STUDIES

This study was approved by the Institutional Review Board Committee at the National Center for Child health and Development, and performed after obtaining informed consent.

Methylation analysis

We first performed bisulfite sequencing for the *H19*-DMR (differentially methylated region) and KvDMR1 as a screening of BWS[11,12] and that for the IG-DMR and the *MEG3*-DMR as a screening of upd(14)pat,[10] using leukocyte genomic DNA. Paternally derived clones were predominantly identified for the four DMRs examined (Figure 1a). We next performed combined bisulfite restriction analysis for multiple DMRs, as reported previously.[13] All the autosomal DMRs exhibited markedly skewed methylation patterns consistent with predominance of paternally inherited clones, whereas the *XIST*-DMR on the X chromosome showed a normal methylation pattern (Figure 1a).

Genome-wide microsatellite analysis

Microsatellite analysis was performed for 90 loci with high heterozygosities in the Japanese population.[14] Major peaks consistent with paternal uniparental isodisomy and minor peaks of maternal origin were identified for at least one locus on each chromosome, with the minor peaks of maternal origin being more obvious in tongue and tonsil tissues than in leukocytes (Figure 1b and Supplementary Table 2). There were no loci with three or four peaks indicative of chimerism. The frequency of the androgenetic cells was calculated as 91% in leukocytes, 70% in tongue cells and 79% in tonsil cells, although the estimation apparently was a rough one (for details, see Supplementary Methods).

Expression analysis

We examined *SNRPN* expression, because *SNRPN* showed strong expression in leukocytes (for details, see Supplementary Data). *SNRPN* expression was almost doubled in the leukocytes of this patient (Figure 1c).

DISCUSSION

These results suggest that this patient had an androgenetic 46,XX cell lineage and a normal 46,XX cell lineage. In this regard, both the androgenetic and the biparental cell lineages appear to have derived from a single sperm and a single ovum, because a single haploid genome of paternal origin and that of maternal origin were identified in this patient by genome-wide microsatellite analysis. Thus, it is likely that after a normal fertilization between an ovum and a sperm, the paternally derived pronucleus alone, but not the maternally derived pronucleus, underwent a mitotic division, resulting both in the generation of the androgenetic cell lineage by endoreplication of

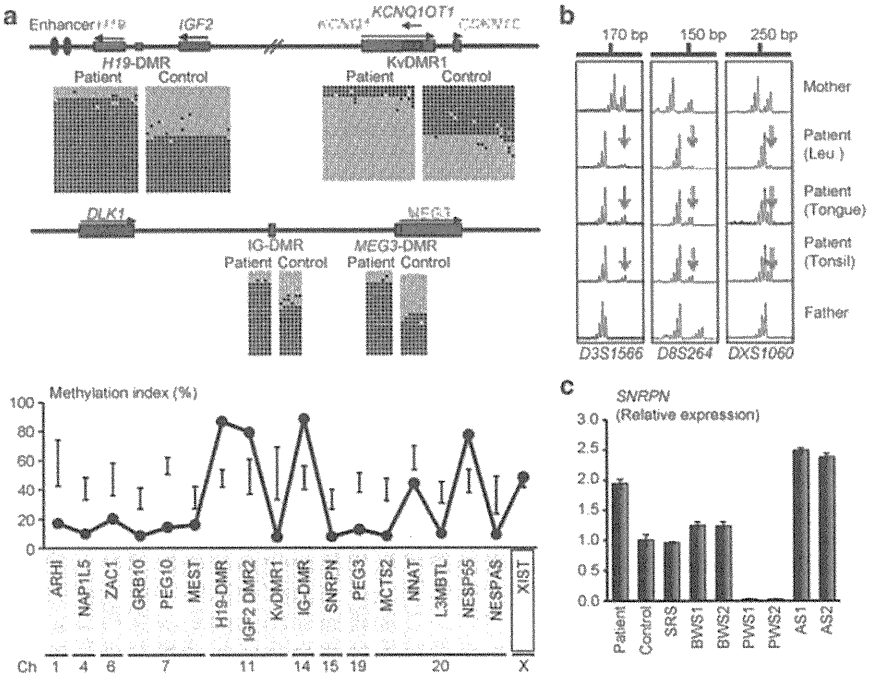

Figure 1 Representative molecular results. (**a**) Methylation analysis. Upper part: Bisulfite sequencing data for the *H19*-DMR and the KvDMR1 on 11p15.5, and those for the IG-DMR and the *MEG3*-DMR on 14q32.2. Each line indicates a single clone, and each circle denotes a CpG dinucleotide; filled and open circles represent methylated and unmethylated cytosines, respectively. Paternally expressed genes are shown in blue, maternally expressed gene in red, and the DMRs in green. The *H19*-DMR, the IG-DMR, and the *MEG3*-DMR are usually methylated after paternal transmission and unmethylated after maternal transmission, whereas the KvDMR1 is usually unmethylated after paternal transmission and methylated after maternal transmission.[10,11] Lower part: Methylation indices (the ratios of methylated clones) obtained from the COBRA analyses for the 18 DMRs. The DMRs highlighted in blue and pink are methylated after paternal and maternal transmissions, respectively. The black vertical bars indicate the reference data (maximum – minimum) in leukocyte genomic DNA of 20 normal control subjects (the *XIST*-DMR data are obtained from 16 control females). (**b**) Representative microsatellite analysis. Major peaks of paternal origin and minor peaks of maternal origin (red arrows) have been identified in this patient. The minor peaks of maternal origin are more obvious in tongue and tonsil tissues than in leukocytes (Leu.). (**c**) Relative expression level (mean ± s.d.) of *SNRPN*. The data are normalized against *TBP*. SRS: an SRS patient with an epimutation (hypomethylation) of the *H19*-DMR; BWS1: a BWS patient with an epimutation (hypermethylation) of the *H19*-DMR; BWS2: a BWS patient with upd(11)pat; PWS1: a Prader-Willi syndrome (PWS) patient with upd(15)mat; PWS2: a PWS patient with an epimutation (hypermethylation) of the *SNRPN*-DMR; AS1: an Angelman syndrome (AS) patient with upd(15)pat; and AS2: an AS patient with an epimutation (hypomethylation) of the *SNRPN*-DMR. The data were obtained using an ABI Prism 7000 Sequence Detection System (Applied Biosystems).

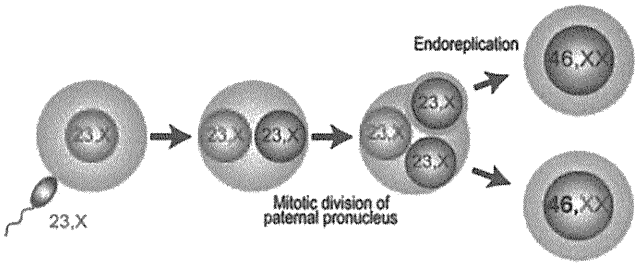

Figure 2 Schematic representation of the generation of the androgenetic/biparental mosaicism. Polar bodies are not shown.

one blastomere containing a paternally derived pronucleus and in the formation of the normal cell lineage by union of paternally and maternally derived pronuclei (Figure 2). This model has been proposed for androgenetic/biparental mosaicism generated after fertilization between a single ovum and a single sperm.[5,15,16] The normal methylation pattern of the *XIST*-DMR is explained by assuming that the two X chromosomes in the androgenetic cell lineage undergo random X-inactivation, as in the normal cell lineage. Furthermore, the results of microsatellite analysis imply that the androgenetic cells were more prevalent in leukocytes than in tongue and tonsil tissues.

A somatic androgenetic cell lineage has been identified in seven liveborn patients including this patient (Supplementary Table 1).[3–7] In this context, leukocytes are preferentially utilized for genetic analyses in human patients, and detailed examinations such as analyses of plural DMRs are necessary to detect an androgenetic cell lineage. Thus, the hitherto identified patients would be limited to those who had androgenetic cells as a predominant cell lineage in leukocytes probably because of a stochastic event and received detailed molecular studies. If so, an androgenetic cell lineage may not be so rare, and could be revealed by detailed analyses as well as examinations of additional tissues in patients with relatively complex phenotypes, as observed in the present patient.

Phenotypic features in androgenetic/biparental mosaicism would be determined by several factors. They include (1) the ratio of two cell lineages in various tissues/organs, (2) the number of imprinted domains relevant to specific features (for example, dysregulation of the imprinted domains on 11p15.5 and 14q32.2 is involved in placentomegaly[9,17]), (3) the degree of clinical effects of dysregulated imprinted domains (an (epi)dominant effect has been assumed for the 11p15.5 imprinted domains[18]), (4) expression levels of imprinted genes in androgenetic cells (although *SNRPN* expression of this patient was consistent with androgenetic cells being predominant in leukocytes, complicated expression patterns have been identified for several imprinted genes in both androgenetic and parthenogenetic fetal mice, probably because of perturbed *cis*- and *trans*-acting regulatory mechanisms[19]) and (5) unmasking of possible paternally inherited recessive mutation(s) in androgenetic cells. Thus, in this patient, it appears that the extent of overall (epi)genetic aberrations exceeded the threshold level for the development of BWS-like and upd(14)pat-like body and placental phenotypes, but remained below the threshold level for the occurrence of other imprinting disorders or recessive Mendelian disorders.

CONFLICT OF INTEREST

The authors declare no conflict of interest.

ACKNOWLEDGEMENTS

This work was supported by grants from the Ministry of Health, Labor, and Welfare, and the Ministry of Education, Science, Sports and Culture.

1 Surani, M. A., Barton, S. C. & Norris, M. L. Development of reconstituted mouse eggs suggests imprinting of the genome during gametogenesis. *Nature* **308,** 548–550 (1984).
2 McGrath, J. & Solter, D. Completion of mouse embryogenesis requires both the maternal and paternal genomes. *Cell* **37,** 179–183 (1984).
3 Hoban, P. R., Heighway, J., White, G. R., Baker, B., Gardner, J., Birch, J. M. *et al.* Genome-wide loss of maternal alleles in a nephrogenic rest and Wilms' tumour from a BWS patient. *Hum. Genet.* **95,** 651–656 (1995).
4 Bryke, C. R., Garber, A. T. & Israel, J. Evolution of a complex phenotype in a unique patient with a paternal uniparental disomy for every chromosome cell line and a normal biparental inheritance cell line. *Am. J. Hum. Genet.* **75**(Suppl), 831 (2004).
5 Giurgea, I., Sanlaville, D., Fournet, J. C., Sempoux, C., Bellanne-Chantelot, C. & Touati, G. Congenital hyperinsulinism and mosaic abnormalities of the ploidy. *J. Med. Genet.* **43,** 248–254 (2006).
6 Wilson, M., Peters, G., Bennetts, B., McGillivray, G., Wu, Z. H., Poon, C. *et al.* The clinical phenotype of mosaicism for genome-wide paternal uniparental disomy: two new reports. *Am. J. Med. Genet. Part A* **146A,** 137–148 (2008).
7 Reed, R. C., Beischel, L., Schoof, J., Johnson, J., Raff, M. L. & Kapur, R. P. Androgenetic/biparental mosaicism in an infant with hepatic mesenchymal hamartoma and placental mesenchymal dysplasia. *Pediatr. Dev. Pathol.* **11,** 377–383 (2008).
8 Jones, K. L. *Smith's Recognizable Patterns of Human Malformation* 6th edn. (Elsevier Saunders: Philadelphia, 2006).
9 Kagami, M., Yamazawa, K., Matsubara, K., Matsuo, N. & Ogata, T. Placentomegaly in paternal uniparental disomy for human chromosome 14. *Placenta* **29,** 760–761 (2008).
10 Kagami, M., Sekita, Y., Nishimura, G., Irie, M., Kato, F., Okada, M. *et al.* Deletions and epimutations affecting the human 14q32.2 imprinted region in individuals with paternal and maternal upd(14)-like phenotypes. *Nat. Genet.* **40,** 237–242 (2008).
11 Yamazawa, K., Kagami, M., Nagai, T., Kondoh, T., Onigata, K., Maeyama, K. *et al.* Molecular and clinical findings and their correlations in Silver-Russell syndrome: implications for a positive role of IGF2 in growth determination and differential imprinting regulation of the IGF2-H19 domain in bodies and placentas. *J. Mol. Med.* **86,** 1171–1181 (2008).
12 Weksberg, R., Shuman, C. & Beckwith, J. B. Beckwith-Wiedemann syndrome. *Eur. J. Hum. Genet.* **18,** 8–14 (2010).
13 Yamazawa, K., Nakabayashi, K., Kagami, M., Sato, T., Saitoh, S., Horikawa, R. *et al.* Parthenogenetic chimaerism/mosaicism with a Silver-Russell syndrome-like phenotype. *J. Med. Genet.* **47,** 782–785 (2010).
14 Ikari, K., Onda, H., Furushima, K., Maeda, S., Harata, S. & Takeda, J. Establishment of an optimized set of 406 microsatellite markers covering the whole genome for the Japanese population. *J. Hum. Genet.* **46,** 207–210 (2001).
15 Kaiser-Rogers, K. A., McFadden, D. E., Livasy, C. A., Dansereau, J., Jiang, R., Knops, J. F. *et al.* Androgenetic/biparental mosaicism causes placental mesenchymal dysplasia. *J. Med. Genet.* **43,** 187–192 (2006).
16 Kotzot, D. Complex and segmental uniparental disomy updated. *J. Med. Genet.* **45,** 545–556 (2008).
17 Monk, D., Arnaud, P., Apostolidou, S., Hills, F. A., Kelsey, G., Stanier, P. *et al.* Limited evolutionary conservation of imprinting in the human placenta. *Proc. Natl. Acad. Sci. USA.* **103,** 6623–6628 (2006).
18 Azzi, S., Rossignol, S., Steunou, V., Sas, T., Thibaud, N., Danton, F. *et al.* Multilocus methylation analysis in a large cohort of 11p15-related foetal growth disorders (Russell Silver and Beckwith Wiedemann syndromes) reveals simultaneous loss of methylation at paternal and maternal imprinted loci. *Hum. Mol. Genet.* **18,** 4724–4733 (2009).
19 Ogawa, H., Wu, Q., Komiyama, J., Obata, Y. & Kono, T. Disruption of parental-specific expression of imprinted genes in uniparental fetuses. *FEBS Lett.* **580,** 5377–5384 (2006).

Supplementary Information accompanies the paper on Journal of Human Genetics website (http://www.nature.com/jhg)

OPEN ACCESS Freely available online

PLoS one

Mamld1 Knockdown Reduces Testosterone Production and *Cyp17a1* Expression in Mouse Leydig Tumor Cells

Michiko Nakamura[1,2], Maki Fukami[1], Fumihiro Sugawa[1], Mami Miyado[1], Katsuya Nonomura[2], Tsutomu Ogata[1]*

1 Department of Molecular Endocrinology, National Research Institute for Child Health and Development, Tokyo, Japan, **2** Department of Renal and Genitourinary Surgery, Hokkaido University Graduate School of Medicine, Sapporo, Japan

Abstract

Background: *MAMLD1* is known to be a causative gene for hypospadias. Although previous studies have indicated that *MAMLD1* mutations result in hypospadias primarily because of compromised testosterone production around the critical period for fetal sex development, the underlying mechanism(s) remains to be clarified. Furthermore, although functional studies have indicated a transactivation function of *MAMLD1* for the non-canonical Notch target *Hes3*, its relevance to testosterone production remains unknown. To examine these matters, we performed *Mamld1* knockdown experiments.

Methodology/Principal Findings: *Mamld1* knockdown was performed with two siRNAs, using mouse Leydig tumor cells (MLTCs). *Mamld1* knockdown did not influence the concentrations of pregnenolone and progesterone but significantly reduced those of 17-OH pregnenolone, 17-OH progesterone, dehydroepiandrosterone, androstenedione, and testosterone in the culture media. Furthermore, *Mamld1* knockdown significantly decreased *Cyp17a1* expression, but did not affect expressions of other genes involved in testosterone biosynthesis as well as in insulin-like 3 production. *Hes3* expression was not significantly altered. In addition, while 47 genes were significantly up-regulated (fold change >2.0×) and 38 genes were significantly down-regulated (fold change <0.5×), none of them was known to be involved in testosterone production. Cell proliferation analysis revealed no evidence for compromised proliferation of siRNA-transfected MLTCs.

Conclusions/Significance: The results, in conjunction with the previous data, imply that *Mamld1* enhances *Cyp17a1* expression primarily in Leydig cells and permit to produce a sufficient amount of testosterone for male sex development, independently of the *Hes3*-related non-canonical Notch signaling.

Citation: Nakamura M, Fukami M, Sugawa F, Miyado M, Nonomura K, et al. (2011) *Mamld1* Knockdown Reduces Testosterone Production and *Cyp17a1* Expression in Mouse Leydig Tumor Cells. PLoS ONE 6(4): e19123. doi:10.1371/journal.pone.0019123

Editor: Michael Polymenis, Texas A&M University, United States of America

Received January 31, 2011; **Accepted** March 17, 2011; **Published** April 29, 2011

Funding: Grant for Research on Intractable Diseases (H22-98) from the Ministry of Health, Labor and Welfare (http://www.mhlw.go.jp/english/), and Grants-in-Aid for Scientific Research (B) (20390265) and for Young Scientists (B-22791715) from the Japan Society for the Promotion of Science (JSPS) (http://www.jsps.go.jp/english/), and by Grant-in-Aid for Scientific Research on Innovative Areas (22132004 A01) from the Ministry of Education, Culture, Sports, Science and Technology (MEXT) (http://www.mext.go.jp/english/). The funders had no role in study design, data collection and analysis, decision to publish, or preparation of the manuscript.

Competing Interests: The authors have declared that no competing interests exist.

* E-mail: tomogata@nch.go.jp

Introduction

MAMLD1 (mastermind-like domain containing 1, alias *CXorf6*) on human chromosome Xq28 is a causative gene for hypospadias, a mild form of 46,XY disorders of sex development (DSD) [1]. To date, multiple mutations have been identified in patients with various types of hypospadias [1–3]. In this regard, the mouse homologous gene *Mamld1* is transiently expressed in fetal Sertoli and Leydig cells around the critical period for sex development [1], and transient *Mamld1* knockdown using small interfering RNAs (siRNAs) reduces testosterone (T) production in cultured mouse Leydig tumor cells (MLTCs) [4]. Furthermore, the upstream region of *MAMLD1/Mamld1* harbors a putative binding site "CCAAGGTCA" for *NR5A1* (alias, *SF-1* and *AD4BP*) [4] that regulates the transcription of a vast array of genes involved in sex development [5], and NR5A1 protein has been shown to bind to the putative target site and exert a transactivation function for *Mamld1* [4]. These findings imply that *MAMLD1/Mamld1* is involved in fetal T production under the regulation of NR5A1, and that *MAMLD1* mutations result in hypospadias primarily because of compromised T production around the critical period for sex development.

However, the underlying mechanism(s) by which impaired *MAMLD1/Mamld1* leads to compromised T production remains to be clarified, although there are several possibilities such as defective activities of enzyme(s) involved in T production and compromised proliferation of Leydig cells. Furthermore, although previous functional studies have indicated that *MAMLD1* has a transactivation function for the non-canonical Notch target *Hes3* [4], its relevance to biological function including T production remains unknown. To examine these matters, we performed detailed analyses in *Mamld1* knockdown experiments using MLTCs.

Methods

Knockdown experiments

MLTCs (ATCC, CRL-2065™) were maintained in RPMI 1640 supplemented with 10% fetal bovine serum, and were

transiently transfected with two siRNAs, i.e., siRNA1 (sense: GCUUCCAGUUCAGAUGCCATT; and anti-sense: UGGCAUCUGAACUGGAAGCTT) and siRNA2 (sense: GGAACUAACCAAAAUUCAATT; and anti-sense: UUGAAUUUUGGUUAGUUCCTC) or with non-targeting control RNA (4611G) (final concentration 20 nM), using Lipofectamine RNAiMAX (Life Technologies). Relative amount of endogenous *Mamld1* mRNA against *B2m* (β2-microglobulin) was determined by the TaqMan real-time PCR method using the probe-primer mix on ABI PRISM 7000 (Life Technologies) (Assay No.: Mm01293665_m1 for *Mamld1*; and Mm00437762_m1 for *B2m*).

Steroid metabolite measurements

MLTCs are known to have the capacity to produce T primarily via Δ^4-pathway, although the amount of T production remains small primarily because of low 17α-hydroxylase and Hsd17b3 activities [6]. MLTCs are also known to retain responsiveness to human chorionic gonadotropin (hCG) [6–8]. Thus, after 48 hours of incubation of transfected MLTCs in 12-well plates with 1 ml of culture medium (an initial cell count: 1×10^5 cells/well), hCG (Mochida Pharmaceutical) was added to the media at a final concentration of 50 IU/L, and the culture media were obtained at one hour after the addition of hCG. Subsequently, steroid metabolites in the T production pathway were measured by the liquid chromatography-tandem mass spectrometry (ASKA Pharma Medical). This experiment was performed three times.

Gene expression analyses

Real-time reverse transcriptase (RT)-PCR and microarray analyses were performed using total RNA extracted from MLTCs that were harvested at the time of steroid metabolite measurements. For real-time RT-PCR analysis, 1 μg of total RNA was examined for relative mRNA dosage against *B2m* by the TaqMan Gene Expression Assay on ABI PRISM 7000 (Assay No.: Mm00446826_m 1 for *Nr5a1* (*Sf1*); Mm00441558_m1 for *Star*; Mm00490735_m1 for *Cyp11a1*; Mm01261921_mH for *Hsd3b1*; and Mm00484040_m1 for *Cyp17a1*). In addition to the genes for steroidogenic enzymes involved in T biosynthesis, we also studied *Insl3* (Mm01340353_m1) for gubernacular development that is expressed in Leydig cells [9,10]. This experiment was repeated three times. For microarray analysis, 300 ng of total RNA was converted into cRNA associated with Cyanine-3 labeled CTP using RNA Spike-In Kit and Quick Amp Labeling Kit, and was subjected to hybridization on Whole Mouse Genome Oligo Microarray in triplicate (4×44 K G4122F) (Agilent Technologies). Subsequently, fluorescent signals were detected by Agilent Scanner, and were analyzed by GeneSpring GX10 (Tomy Digital Biology). The microarray data have been deposited in NCBI's Gene Expression Omnibus and are accessible through GEO series accession number GSE26913 (http://www.ncbi.nlm.nih.gov/geo/query/acc.cgi?acc=GSE26913). All data is MIAME compliant and the raw data has been deposited in a MIAME compliant database (GEO), as detailed on the MGED Society website (http://www.mged.org/Workgroups/MIAME/miame.html).

Cell proliferation assays

The number of viable MLTCs transfected with two siRNAs or with non-targeting RNA was calculated by the colorimetric method [11,12], using CellTiter 96 AQueous One Solution Cell Proliferation Assay (Promega). The detailed procedure has been described in the manufacturer's protocol. In brief, MLTCs were cultured in 96-well plates (an initial cell count: 1×10^4 cells/well), and the cell number was determined every 24 hours by measuring the absorbance on a plate reader (Molecular Device) at 490 nm. This method is based on a positive correlation between the number of viable cells and the absorbance until the cells become confluent, and our preliminary studies showed a good correlation until the absorbance of ~2.0 (~6×10^5 cells/well) (Figure S1). This experiment was performed three times.

Statistical analysis

Statistical significance was examined by Student's *t*-test or by Mann-Whitney's *U*-test. $P<0.05$ was considered significant.

Results

Steroid metabolite measurements

The mean steroid metabolite concentrations are shown in Figure 1, together with the mean endogenous *Mamld1* mRNA levels that were markedly reduced in both siRNA1- and siRNA2-transfected MLTCs at the time of steroid metabolite measurements. The concentrations of pregnenolone and progesterone remained comparable between the culture media with siRNA-transfected MLTCs and those with non-targeted MLTCs, whereas the concentrations of 17-OH pregnenolone, 17-OH progesterone, dehydroepiandrosterone, androstenedione, and T were significantly lower in the culture media with siRNA-transfected MLTCs than in those with non-targeted MLTCs. Furthermore, comparison of the steroid metabolite concentrations in the media with non-targeted MLTCs confirmed revealed the Δ^4-pathway dominant T production, markedly low 17α-hydroxylase activity and well preserved 17/20 lyase activity for both Δ^4- and Δ^5-pathways, and extremely low Hsd17b3 activity in MLTCs. These results indicated that *Mamld1* knockdown further reduced 17α-hydroxylase activity that was originally low in MLTCs.

Gene expression analyses

Real-time RT-PCR and microarray analyses showed significantly decreased *Cyp17a1* expression (~70%) in both siRNA1- and siRNA2-transfected MLTCs (Figure 2). Although *Cyp11a1* and *Hsd3b1* expressions were found to be reduced in siRNA1-transfected MLTCs by real-time RT-PCR and microarray analyses respectively, such reduced activities were not reproduced in siRNA2-transfected MLTCs. The siRNAs knockdown did not affect the expressions of *Nr5a1* (*Sf1*), *Star*, *Por*, and *Insl3*. The assessment of *Hsb17b3* was impossible, because of its extremely low expression.

In addition, 47 genes including a Notch-related gene *Hey1* were significantly up-regulated (fold change >2.0×) and 38 genes were significantly down-regulated (fold change <0.5×) in both siRNA1- and siRNA2-transfected MLTCs (Table S1 and Table S2). However, *Mamld1* knockdown had no discernible effect on the *Hes3* expression level (siRNA1: fold change 0.92, $P=0.80$; siRNA2: fold change 1.43, $P=0.35$). The microarray data have been deposited in NCBI's Gene Expression Omnibus and are accessible through GEO series accession number GSE26913 (http://www.ncbi.nlm.nih.gov/geo/query/acc.cgi?acc=GSE26913).

Cell proliferation assays

The results are shown in Figure 3. The mean endogenous *Mamld1* mRNA levels were sufficiently suppressed for 120 hours in both siRNA1- and siRNA2-transfected MLTCs. Under this condition, the absorbance values for the siRNA-targeted and non-targeted MLTCs showed a roughly linear increase until 72 hours (absorbance ~2.0). In this linear proliferative phase, although the absorbance values were significantly decreased in siRNA2-treated MLTCs at 24 and 48 hours after the transfection,

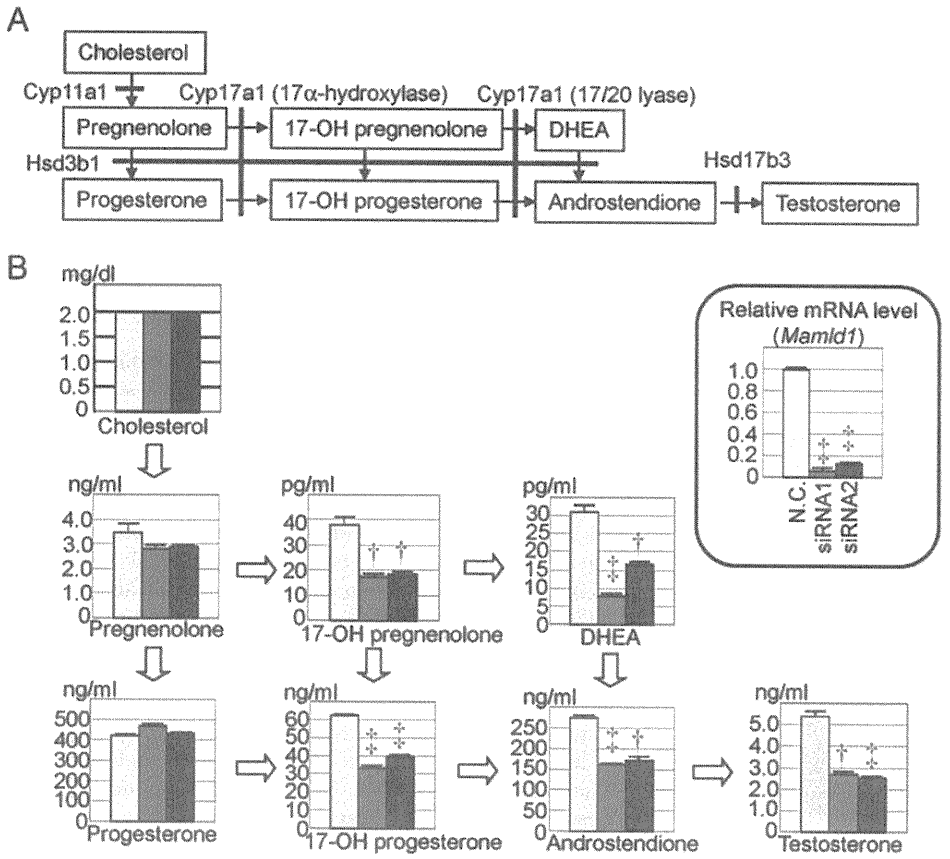

Figure 1. Steroid metabolite concentrations. A. Steroid metabolic pathway from cholesterol to testosterone and enzymes involved in each conversion. Pregnenolone, 17-OH pregnenolone, and DHEA (dehydroepiandrosterone) are Δ^4-steroid metabolites (Δ^4-pathway), and progesterone, 17-OH progesterone, and androstenedione are Δ^5-steroid metabolites (Δ^5-pathway). Hsd3b1 also functions as $\Delta^{5\,4}$ isomerase. B. Steroid metabolite concentrations in culture media and endogenous *Mamld1* expression levels in MLTCs. The yellow, the green, and the blue bars indicate the data obtained from MLTCs transfected with non-targeting RNA, siRNA1, and siRNA2, respectively. †: $P<0.01$; and ‡: $P<0.001$. The conversion factor to the SI unit: cholesterol 0.026 (mmol/L), pregnenolone 3.16 (nmol/L), progesterone 3.18 (nmol/L), 17-OH pregnenolone 3.00 (pmol/L), 17-OH progesterone 3.03 (nmol/L), DHEA 3.46 (pmol/L), androstenedione 3.49 (nmol/L), and testosterone 3.46 (nmol/L).
doi:10.1371/journal.pone.0019123.g001

this was not reproduced in siRNA1-transfected MLTCs. After 72 hours of incubation, the MLTCs became confluent, and the absorbance values became a plateau phase around ~2.0. In this plateau phase, although the absorbance values at 96 hours after the transfection were significantly low in both siRNA1- and siRNA2-treated MLTCs, this was not reproduced at 120 hours after the transfection.

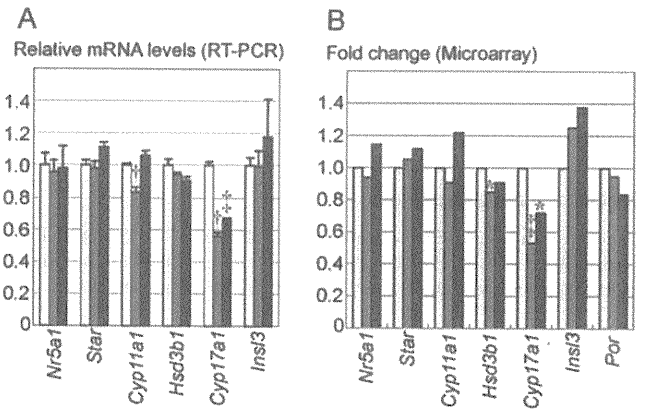

Figure 2. Gene expression analysis. The yellow, the green, and the blue bars indicate the data obtained from MLTCs transfected with non-targeting RNA, siRNA1, and siRNA2, respectively. *: $P<0.05$; †: $P<0.01$; and ‡: $P<0.001$. A. Real-time RT-PCR analysis. B. Microarray analysis.
doi:10.1371/journal.pone.0019123.g002

Discussion

Mamld1 knockdown with two siRNAs resulted in compromised T production, together with reduced 17α-hydroxylase activity and *Cyp17a1* expression in MLTCs. This provides further support for a positive role of *Mamld1* in T production [4], and implies for the first time a possible interaction between *Mamld1* and *Cyp17a1*, at least in MLTCs. In this regard, it is noteworthy that *Mamld1* is clearly expressed in fetal Leydig and Sertoli cells and is barely expressed in adrenal cells [1,13], and that *Cyp17a1* expression is indispensable for T production in Leydig cells [14]. Thus, it appears likely that *Mamld1* enhances *Cyp17a1* expression primarily in Leydig cells, permitting the production of a sufficient amount of T for male sex development. In addition, since the expressions of other genes involved in T production and insulin-like 3 biosynthesis were not clearly affected in siRNA-transfected MLTCs, this would argue against the possibility that *Mamld1* knockdown causes a global dysfunction of MLTCs, resulting in T hyposecretion.

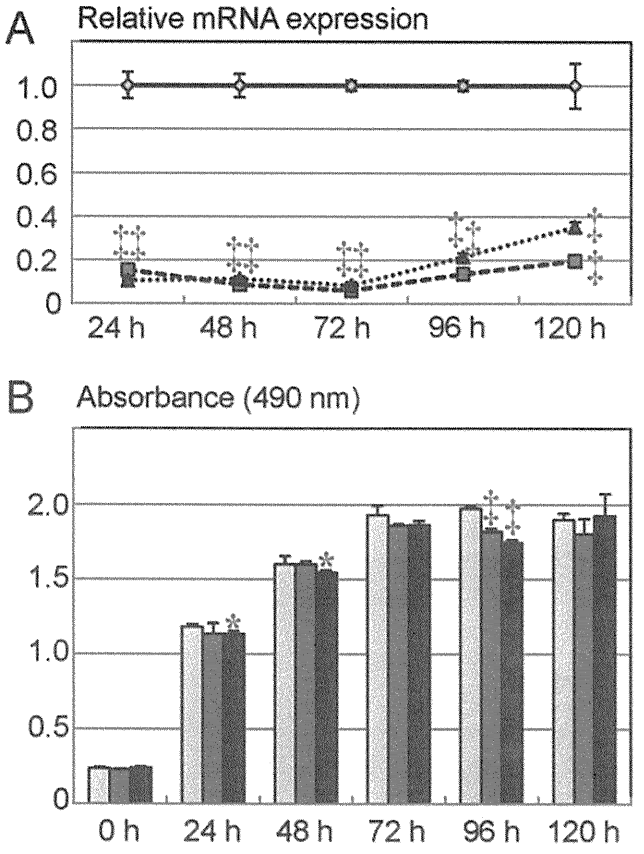

Figure 3. Cell proliferation assay. The yellow, the green, and the blue line graphs and bars indicate the data obtained from MLTCs transfected with non-targeting RNA, siRNA1, and siRNA2, respectively. *: $P<0.05$; and ‡: $P<0.001$. A. Endogenous *Mamld1* expression levels. B. Absorbance values.
doi:10.1371/journal.pone.0019123.g003

However, a straightforward explanation appears to be difficult between impaired 17α-hydroxylase activity and reduced *Cyp17a1* expression. Indeed, 17/20 lyase activity was well preserved in siRNA-transfected MLTCs, although the same Cyp17a1 enzyme is utilized for both17α-hydroxylase and 17/20 lyase reactions [14]. In addition, defective 17α-hydroxylase activity occurred in the presence of ~70% of *Cyp17a1* expression, despite 17α-hydroxylase deficiency being an autosomal recessive disease in which 50% of enzyme reduction has no major effect on the steroid metabolism [14]. In this context, it is notable that MLTCs originally have a markedly low 17α-hydroxylase activity and a well preserved 17/20 lyase activity for both Δ^4- and Δ^5-pathways (Figure 1) [6]. Such a unique property of MLTCs may be relevant to the preferential impairment of 17α-hydroxylase activity in siRNA-transfected MLTCs.

Mamld1 knockdown had no discernible effect on the *Hes3* expression. In addition, while a Notch-related gene *Hey1* [15–17] was up-regulated in siRNA-transfected MLTCs, there are no data suggesting a possible interaction between *Hes3* and *Hey1* in the T production process. Furthermore, while *Hes3* is weakly expressed in the MLTCs [4], *Hes3* expression is apparently absent from mouse fetal gonads around the critical period for sex development [18]. Thus, it is unlikely that *Hes3*-related non-canonical Notch signaling underlies a link between *Mamld1* and *Cyp17a1*. In addition, while microarray analysis revealed multiple up-regulated and down-regulated genes in siRNA-transfected MLTCs, none of them is known to be involved in the T production at present. It remains to be clarified, therefore, how *Mamld1* enhances *Cyp17a1* expression and T production.

The cell proliferation analysis revealed no clear evidence for the reduced number of viable MLTCs transfected with siRNAs. This implies that the reduced T and several other steroid metabolite concentrations observed at 48 hours after the transfection (Figure 1) are inexplicable by impaired proliferation of MLTCs. However, since the cell doubling time of MLTCs is 35–40 hours [8], a slight difference in cell proliferation would not be detected by the present analysis. Thus, it might remain tenable at this time that impaired cell proliferation becomes discernible after multiple cell divisions, and that such a possibly reduced cell proliferation underlies the development of hypospadias phenotype in patients with *MAMLD1* mutations, in addition to compromised T production in Leydig cells.

In summary, the present study implies that *Mamld1* enhances *Cyp17a1* expression primarily in Leydig cells and permit to produce a sufficient amount of T for male sex development, independently of the *Hes3*-related non-canonical Notch signaling. Although the data were obtained from *in vitro* studies using MLTCs, they provides a useful clue to clarify the underlying factors for the development of hypospadias and other forms of 46,XY DSD.

Supporting Information

Figure S1 Cell proliferation assay by the colorimetric method, using non-transfected MLTCs. The absorbance value is well correlated with cell number until the absorbance value of ~2.0, but does not reflect the cell number after the absorbance value of ~2.0.
(TIF)

Table S1 List of up-regulated genes in MLTCs trasnfected with siRNAs for *Mamld1*.
(DOC)

Table S2 List of down-regulated genes in MLTCs trasnfected with siRNAs for *Mamld1*.
(DOC)

Author Contributions

Conceived and designed the experiments: MF KN TO. Performed the experiments: MN MF FS MM. Analyzed the data: MN MF. Contributed reagents/materials/analysis tools: MF TO. Wrote the paper: TO.

References

1. Fukami M, Wada Y, Miyabayashi K, Nishino I, Hasegawa T, et al. (2006) CXorf6 is a causative gene for hypospadias. Nat Genet 38: 1369–1371.
2. Kalfa N, Liu B, Klein O, Audran F, Wang MH, et al. (2008) Mutations of CXorf6 are associated with a range of severities of hypospadias. Eur J Endocrinol 159: 453–458.
3. Chen Y, Thai HT, Lundin J, Lagerstedt-Robinson K, Zhao S, et al. (2010) Mutational study of the MAMLD1-gene in hypospadias. Eur J Med Genet 53: 122–126.
4. Fukami M, Wada Y, Okada M, Kato F, Katsumata N, et al. (2008) Mastermind-like domain-containing 1 (MAMLD1 or CXorf6) transactivates the Hes3 promoter, augments testosterone production, and contains the SF1 target sequence. J Biol Chem 283: 5525–5532.
5. Lin L, Achermann JC (2008) Steroidogenic factor-1 (SF-1, Ad4BP, NR5A1) and disorders of testis development. Sex Dev 2: 200–209.
6. Panesar NS, Chan KW, Ho CS (2003) Mouse Leydig tumor cells produce C-19 steroids, including testosterone. Steroids 68: 245–251.

7. Ascoli M, Puett D (1978) Gonadotropin binding and stimulation of steroidogenesis in Leydig tumor cells. Proc Natl Acad Sci U S A 75: 99–102.
8. Rebois RV (1982) Establishment of gonadotropin-responsive murine leydig tumor cell line. J Cell Biol 94: 70–76.
9. Hughes IA, Acerini CL (2008) Factors controlling testis descent. Eur J Endocrinol 159 Suppl 1: S75–82.
10. Nef S, Parada LF (1999) Cryptorchidism in mice mutant for Insl3. Nat Genet 22: 295–299.
11. Berridge MV, Tan AS (1993) Characterization of the cellular reduction of 3-(4,5-dimethylthiazol-2-yl)-2,5-diphenyltetrazolium bromide (MTT): subcellular localization, substrate dependence, and involvement of mitochondrial electron transport in MTT reduction. Arch Biochem Biophys 303: 474–482.
12. Cory AH, Owen TC, Barltrop JA, Cory JG (1991) Use of an aqueous soluble tetrazolium/formazan assay for cell growth assays in culture. Cancer Commun 3: 207–212.
13. Ogata T, Laporte J, Fukami M (2009) MAMLD1 (CXorf6): a new gene involved in hypospadias. Horm Res 71: 245–252.
14. Achermann JC, Hughes IA (2008) Disorders of sex development. In: Kronenberg HM, Melmed M, Polonsky KS, Larsen PR, eds. Williams textbook of endocrinology, 11th editions Philadelphia: Saunders. pp 783–848.
15. Bolos V, Grego-Bessa J, de la Pompa JL (2007) Notch signaling in development and cancer. Endocr Rev 28: 339–363.
16. Katoh M (2007) Integrative genomic analyses on HES/HEY family: Notch-independent HES1, HES3 transcription in undifferentiated ES cells, and Notch-dependent HES1, HES5, HEY1, HEY2, HEYL transcription in fetal tissues, adult tissues, or cancer. Int J Oncol 31: 461–466.
17. Kageyama R, Ohtsuka T, Kobayashi T (2007) The Hes gene family: repressors and oscillators that orchestrate embryogenesis. Development 134: 1243–1251.
18. Tang H, Brennan J, Karl J, Hamada Y, Raetzman L, et al. (2008) Notch signaling maintains Leydig progenitor cells in the mouse testis. Development 135: 3745–3753.

Journal of Human Genetics (2011) 56, 566–571

www.nature.com/jhg

ORIGINAL ARTICLE

Maternal age effect on the development of Prader–Willi syndrome resulting from upd(15)mat through meiosis 1 errors

Keiko Matsubara[1,2,3], Nobuyuki Murakami[2,3], Toshiro Nagai[2] and Tsutomu Ogata[1]

Prader–Willi syndrome (PWS) is primarily caused by deletions involving the paternally derived imprinted region at chromosome 15q11.2–q13 and maternal uniparental disomy 15 (upd(15)mat). The underlying mechanisms for upd(15)mat include trisomy rescue (TR), gamete complementation (GC), monosomy rescue and post-fertilization mitotic error, and TR/GC is mediated by non-disjunction at maternal meiosis 1 (M1) or meiosis 2 (M2). Of these factors involved in the development of upd(15)mat, M1 non-disjunction is a maternal age-dependent phenomenon. We studied 117 Japanese patients with PWS and identified deletions in 84 patients (Deletion group) and TR/GC type upd(15)mat through M1 non-disjunction in 15 patients (TR/GC (M1) group), together with other types of abnormalities. Maternal age was significantly higher in TR/GC (M1) group than in Deletion group (median (range), 37 (35–45) versus 30 (19–42); $P=1.0\times10^{-7}$). Furthermore, delayed childbearing age became obvious since the year 2003 in Japan, and relative frequency of TR/GC (M1) group was significantly larger in patients born since the year 2003 than in those born until the year 2002. The results imply that the advanced maternal age at childbirth is a predisposing factor for the development of upd(15)mat because of increased M1 errors.
Journal of Human Genetics (2011) **56**, 566–571; doi:10.1038/jhg.2011.59; published online 2 June 2011

Keywords: maternal age effect; meiosis 1; non-disjunction; Prader-Willi syndrome; upd(15)mat

INTRODUCTION

Prader–Willi syndrome (PWS) is a developmental disorder associated with various dysmorphic, neurologic, cognitive, endocrine and behavioral/psychiatric features.[1] It is caused by absent expression of paternally derived genes on the imprinted region at chromosome 15q11.2–q13, and previous studies have indicated that deletions of the paternally derived imprinted region and maternal uniparental disomy 15 (upd(15)mat) account for ~70 and ~25% of PWS patients, respectively.[1] The remaining PWS patients have rare abnormalities such as epimutations (hypermethylation) of the PWS imprinting center (IC), at the differentially methylated region encompassing exon 1 of *SNRPN* and microdeletions involving the PWS-IC or HBII-85 small nucleolar RNAs distal to the PWS-IC.[2–4]

Upd(15)mat are primarily caused by four mechanisms; that is, trisomy rescue (TR), gamete complementation (GC), monosomy rescue (MR) and post-fertilization mitotic error (PE).[5] TR refers to a condition in which chromosome 15 of paternal origin is lost from a zygote with trisomy 15, formed by fertilization between a disomic oocyte and a normal sperm. GC results from fertilization of a disomic oocyte with a nullisomic sperm. MR refers to a condition in which chromosome 15 of maternal origin is replicated in a zygote with monosomy 15, formed by fertilization between a normal oocyte and a nullisomic sperm. PE is an event after formation of a normal zygote. In this regard, a disomic oocyte specific to TR and GC is produced by non-disjunction at meiosis 1 (M1) or meiosis 2 (M2), and non-disjunction at M1 is known to increase with maternal age, probably because of a long-term (10–50 years) meiotic arrest at prophase 1.[6]

It is predicted, therefore, that the relative frequency of TR/GC-type upd(15)mat through M1 non-disjunction is high in PWS patients born to aged mothers and is increasing in countries where childbearing age is rising. In this context, previous studies have revealed a significantly higher maternal age in PWS patients with upd(15)mat than in those with deletions,[7,8] a significantly higher relative frequency of upd(15)mat in patients born to mothers aged $\geqslant$35 years than in those born to mothers aged <35 years[9] and a significantly increased relative frequency of upd(15)mat in PWS patients <5 years of age in United Kingdom where childbearing age is increasing.[10] In these

[1]Department of Molecular Endocrinology, National Research Institute for Child Health and Development, Tokyo, Japan and [2]Department of Pediatrics, Dokkyo Medical University Koshigaya Hospital, Saitama, Japan
[3]These authors contributed equally to this work.
Correspondence: Dr T Ogata, Department of Molecular Endocrinology, National Research Institute for Child Health and Development, 2-10-1 Ohkura, Setagaya, Tokyo 157-8535, Japan.
E-mail: tomogata@nch.go.jp
Received 3 March 2011; revised 29 April 2011; accepted 8 May 2011; published online 2 June 2011

studies, however, as underlying mechanisms for upd(15)mat have not been examined, it remains to be clarified whether such maternal age effect on the occurrence of upd(15)mat is primarily mediated by M1 non-disjunction. Furthermore, after studying underlying mechanisms for upd(15)mat by microsatellite analysis, Robinson *et al.*[11] have mentioned that maternal age effect is similar between M1 and M2 errors. Thus, it remains to be clarified whether advanced maternal age is relevant to the occurrence of TR/GC type upd(15)mat through M1 errors.

Here, we report that the advanced maternal age at childbirth constitutes a risk factor for TR/GC type upd(15)mat through M1 non-disjunction.

MATERIALS AND METHODS

This study was approved by the Institute Review Board Committees at the National Center for Child Health and Development and Dokkyo University Koshigaya Hospital, and performed after obtaining informed consent.

PWS patients

This study consisted of 117 Japanese PWS patients (72 male patients and 45 female patients) who satisfied the following selection criteria: (1) normal karyotype in all the 50 lymphocytes examined, (2) hypermethylated PWS-IC that was confirmed by methylation analysis for bisulfite-treated leukocyte genomic DNA, using methylated and unmethylated allele-specific PCR primers (Supplementary Figure 1),[12] and (3) positive data on the maternal age at childbirth (parental age was not found in two aged patients who had left our follow-up and whose hospital records had been discarded and in one patient who was born after artificial insemination by donor).

Molecular studies

We performed fluorescence *in situ* hybridization analysis, microsatellite analysis and multiplex ligation-dependent probe amplification (MLPA) analysis. For fluorescence *in situ* hybridization analysis, an ~125-kb probe identifying a region encompassing *SNRPN* was hybridized to lymphocyte metaphase spreads, together with a CEP 15 probe for *D15Z1* and a probe for *PML* on 15q22 utilized as internal controls. The probe for the *SNRPN* region was labeled with digoxigenin and detected by rhodamine anti-digoxigenin, and the control probes were detected according to the manufacturer's protocol (Abbott, Chicago, IL, USA). For microsatellite genotyping, PCR amplification was performed for 13 microsatellite loci on chromosome 15, using fluorescently labeled forward primers and unlabeled reverse primers. Subsequently, the PCR products were determined for size on a CEQ8000 autosequencer (Beckman Coulter, Fullerton, CA, USA). For MLPA analysis, we utilized a commercially available MLPA probe mix (ME028-B1) for multiple segments on the chromosome 15 imprinted region, including the PWS-IC and three portions within the HBII-85 small nucleolar RNAs (MRC-Holland, Amsterdam, The Netherlands). The procedure was as described in the manufacturer's instructions. The primers utilized in this study are summarized in Supplementary Table 1.

Classification of PWS patients

The PWS patients were classified into several groups, according to the underlying (epi) genetic causes (Figure 1). In particular, upd(15)mat was divided into three groups by the previously reported methods[13] (Supplementary Figure 2): (1) heterodisomy for at least one of the three adjacent pericentromeric (<4 Mb from the centromere) microsatellite loci (*D15S541*, *D15S542* and *D15S1035*) was regarded as indicative of TR/GC type upd(15)mat through M1 non-disjunction (TR/GC (M1) group), (2) the combination of isodisomy for the pericentromeric microsatellite loci and heterodisomy for at least one middle to distal microsatellite loci was interpreted as indicative of TR/GC type upd(15)mat through M2 non-disjunction (TR/GC (M2) group) and (3) isodisomy for all the informative microsatellite loci was regarded as indicative of MR/PE type upd(15)mat (MR/PE group). However, it is usually impossible to distinguish between TR and GC, and between MR and PE on the basis of microsatellite data, although identification of segmental isodisomy or mosaicism with a normal cell lineage is unique to PE.[14,15]

Analysis of parental ages

We compared parental ages between different groups and between two different time periods (until the year 2002 and since the year 2003), and relative frequency of each group between the two time periods. The setting of the two time periods was based on the Annual Vital Statistics Data from the Japanese Ministry of Health, Labor and Welfare (http://www.mhlw.go.jp/toukei/list/81-1.html). The maternal age producing the largest number of live births changed from 25–29 years to 30–34 years, and that producing the third largest number of live births changed from 20–24 years to 35–39 years, between the two time periods (Supplementary Figure 3).

Statistical significance of the median age was examined by the Mann–Whitneys *U*-test, that of the correlation between parental ages by Spearman's rank correlation test, and that of relative frequency by the Fisher's exact probability test. $P<0.05$ was considered significant.

RESULTS

Classification of PWS patients

The results are shown in Figure 1. Fluorescence *in situ* hybridization analysis revealed heterozygous deletions in 84 of the 117 patients (Supplementary Figure 4;Deletion group). Then, microsatellite genotyping was carried out in 27 of the 33 patients without deletions, classifying 15 patients as TR/GC (M1) group, seven patients as TR/GC (M2) group and three patients as MR/PE group (Figure 2;in the remaining six patients, further studies were refused by the parents). There was no finding indicative of segmental isodisomy or mosaicism. Finally, MLPA was performed in the remaining two non-upd(15)mat patients, identifying no microdeletion affecting the PWS-IC. Thus, the two patients were classified as Epimutation group.

Analysis of parental ages

Distribution of parental ages in each group is shown in Figure 3a, and parental age data are summarized in Table 1. Maternal ages were invariably ⩾35 in TR/GC (M1) group. Furthermore, comparison of maternal ages in Deletion, TR/GC (M1) and TR/GC (M2) groups with >5 patients revealed significant difference between Deletion and TR/GC (M1) groups ($P=1.0\times10^{-7}$), but not between Deletion and TR/GC (M2) groups ($P=0.19$), and between TR/GC (M1) and TR/GC (M2) groups ($P=0.085$). Paternal ages showed similar tendency, with

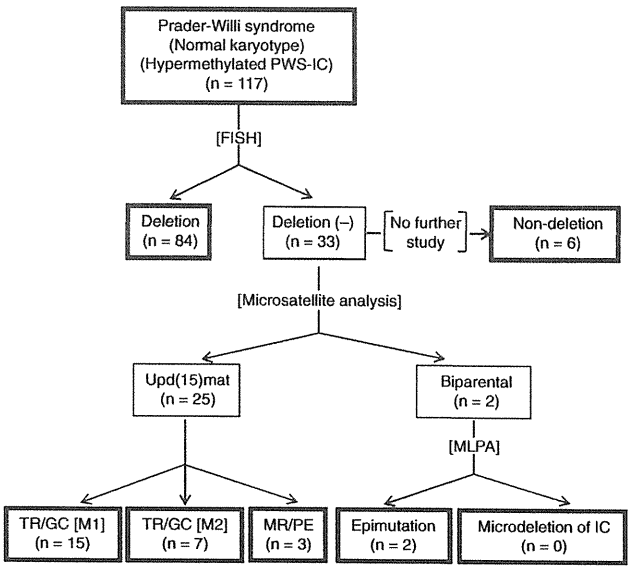

Figure 1 Classification of 117 Japanese patients with Prader–Willi syndrome phenotype.

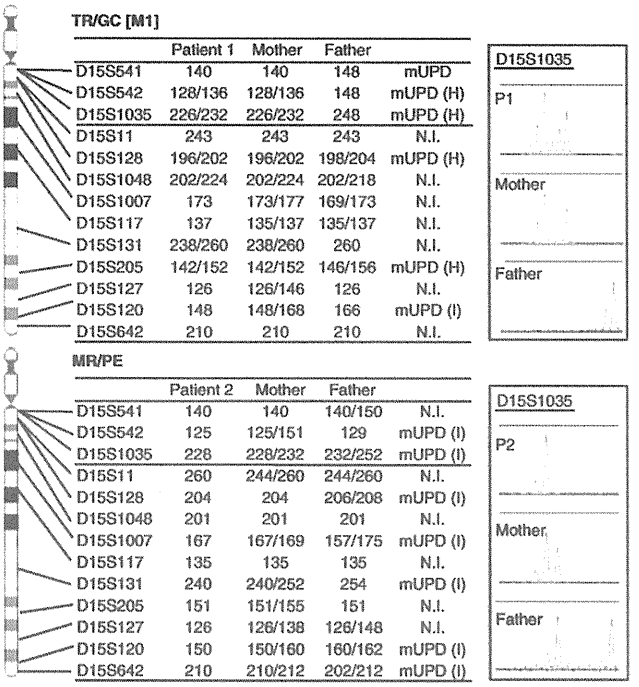

Figure 2 Chromosomal locations of the examined microsatellite loci and representative results. MUPD, maternal uniparental disomy (unknown for heterodisomy or isodisomy); mUPD (H), maternal uniparental heterodisomy; mUPD (I), maternal uniparental isodisomy; N.I., not informative. Pericentromeric loci are present in a heterodisomic status in patient 1, and this is consistent with trisomy rescue/gamete complementation (meiosis 1) (TR/GC (M1)) type maternal uniparental disomy 15 (upd(15)mat). For D15S1035, for example, both of the heterozygous maternal alleles are inherited by patient 1, whereas the homozygous paternal alleles are not transmitted to patient 1; this demonstrates mUPD (H) for this locus. In patient 2, all informative loci are present in an isodisomic condition, and this is compatible with monosomy rescue/post-fertilization mitotic error (MR/PE) type upd(15)mat. For D15S1035, for example, one of the two heterozygous maternal alleles is transmitted to patient 2, whereas both of the heterozygous paternal alleles are not inherited by patient 2; this demonstrates mUPD (I) for this locus.

significant difference between Deletion and TR/GC (M1) groups ($P=8.8\times10^{-5}$), but not between Deletion and TR/GC (M2) groups ($P=0.39$), and between TR/GC (M1) and TR/GC (M2) groups ($P=0.39$). However, whereas a significant correlation was observed between maternal and paternal ages in Deletion and TR/GC (M2) groups, there was no significant correlation between maternal and paternal ages in TR/GC (M1) group because of relatively advanced maternal ages in this group (Figure 3b). In addition, whereas maternal ages at childbirth were grossly similar between Deletion and TR/GC (M2) groups and the Japanese general population (the mean parental ages at childbirth in Japan were based on the data registered in the Ministry of Health, Labor and Welfare; http://www.mhlw.go.jp/toukei/list/81-1.html), they were obviously higher in TR/GC (M1) group than in the Japanese general population. Paternal ages at childbirth were grossly similar between Deletion group and the Japanese general population and tended to be higher in TR/GC (M1) and TR/GC (M2) groups than in the Japanese general population.

Relative frequency of each group markedly differed between 75 patients born until 2002 and 42 patients born since 2003 (Figure 3c). Here, TR/GC (M1) was indicated in three of the 75 patients born until the year 2002, and six non-deletion type patients were invariably born until the year 2002. Thus, TR/GC (M1) group accounted for at least three and up to nine of the 75 patients born until the year 2002, and 12 of the 42 patients born since the year 2003. Thus, the relative frequency of TR/GC (M1) was assessed to be significantly different, with the *P*-values being 1.8×10^{-7} for 3/75 versus 12/42, and 0.025 for 9/75 versus 12/42. In addition, there was no significant change in the parental ages of each group between the two time periods, although the maternal ages at birth of all the patients significantly differed between the two time periods.

DISCUSSION

The present study revealed deletions in 84 patients, upd(15)mat in 25 patients and epimutations in 2 patients. In addition, whereas microsatellite and MLPA analyses were not performed in six patients with non-deletion, the present and the previous studies argue that most of them have upd(15)mat, especially TR/GC (M1) type upd(15)mat.[1,13] Thus, the relative frequency of deletions, upd(15)mat and other rare causes appears to be similar between Japanese patient and previously reported Caucasian patients.[1]

Notably, the present study implies that advanced maternal age at childbirth constitutes a risk factor for the development of TR/GC (M1) type upd(15)mat. Indeed, maternal ages were significantly higher in TR/GC (M1) group than in Deletion group, which is free from maternal age effect. Although a significant difference was not found between maternal age-dependent TR/GC (M1) group and maternal age-independent TR/GC (M2) group, this would primarily be due to the small number of TR/GC (M2) group. Furthermore, the relative frequency of TR/GC (M1) group significantly increased since the year 2003 when delayed childbearing age became obvious, and the advanced maternal ages at birth since the year 2003 were primarily associated with the high frequency of TR/GC (M1) group rather than the advanced maternal ages in each group. Although it was impossible to distinguish between TR and GC, and between MR and PE,[16] this would not pose a major problem. The patients with M1 non-disjunction are included only in TR/GC (M1) group.

Paternal and environmental factors should also be considered for the present results. For a paternal factor, the frequencies of microdeletions and nullisomic sperms might increase with age.[17] However, paternal ages at childbirth in each group were similar between the two time periods, and the relative frequency of Deletion group actually decreased since the year 2003. Furthermore, whereas nullisomic sperms can be a background of the development of GC, concomitant occurrence of a nullisomic sperm and a disomic oocyte must be extremely rare. Rather, nullisomic sperms would primarily constitute an underlying factor for the development of maternal age-independent MR. For an environmental factor, it is predicted that chemical materials are increasing with time and that aged parents are exposed to such materials for a long time. In this regard, it has been reported that exposure to environmental chemicals may exaggerate the occurrence of aneuploidies in females.[18] Thus, the environmental factor might be relevant to the recent increase of TR/GC (M1) group, although it is unlikely that this factor constitutes the major cause of the increased TR/GC (M1) type upd(15)mat. In males, whereas it has been reported that exposure to chemical materials might facilitate the occurrence of PWS, the relative frequency of genetic causes remained unchanged in PWS patients born to such males.[19–21] Collectively, the effects of such non-maternal age factors would remain small, if any, although further careful examinations are required for the precise evaluation of the maternal age effect on the occurrence of TR/GC (M1).

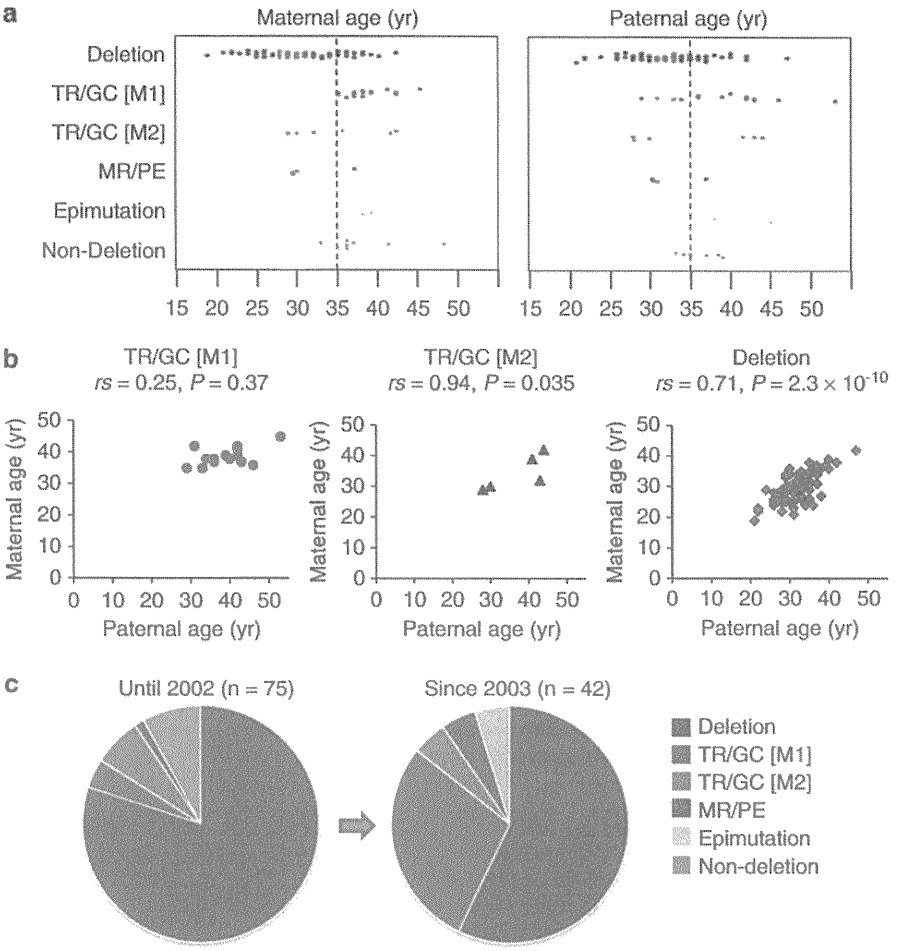

Figure 3 Analysis of parental ages at childbirth. (**a**) The distribution of parental ages in each group. The light pink and blue vertical bars represent the mean maternal and paternal ages at childbirth from the year 1970 to the year 2008. (**b**) Correlation between maternal and paternal ages at childbirth. Significant correlation is observed in trisomy rescue/gamete complementation (meiosis 2) (TR/GC (M2)) and Deletion groups, but not in trisomy rescue/gamete complementation (meiosis 1) (TR/GC (M1)) group because of relatively advanced maternal age. (**c**) Relative frequency of each group in 75 patients born until the year 2002 (n=60, 3, 5, 1, 0 and 6 for Deletion, TR/GC (M1), TR/GC (M2), monosomy rescue/post-fertilization mitotic error (MR/PE), epimutation and non-deletions groups, respectively) and in 42 patients born since the year 2003 (n=24, 12, 2, 2, 2 and 0 for Deletion, TR/GC (M1), TR/GC (M2), MR/PE, Epimutation and Non-deletions groups, respectively).

Several points should be made with regard to the present study. First, we classified upd(15)mat primarily on the basis of the results of three pericentromeric microsatellite loci, with the assumption of no recombination between the centromere and the three loci, as have been employed in the previous study.[13] The methods would be basically acceptable, because the three loci reside within a 4 Mb region from the centromere and a recombination is relatively rare in the centromeric regions.[22] However, it remains possible that a cryptic recombination(s) might have occurred in the pericentromeric region.

Second, upd(15)mat may also be caused by maternal age-dependent meiotic sister chromatid pre-division that can lead to aneuploid oocytes, including disomic oocytes specific to TR/GC.[23] In this regard, as such disomic oocytes can have various patterns of isodisomic and heterodisomic regions, it is impossible to discriminate between upd(15)mat through sister chromatid pre-division and that through conventional meiotic non-disjunction by microsatellite analysis. Thus, the patients classified as TR/GC (M1) group may have upd(15)mat due to maternal age-dependent conventional non-disjunction at M1 and maternal age-dependent sister chromatid pre-division, whereas those classified as TR/GC (M2) group may have upd(15)mat due to maternal age-independent conventional non-disjunction at M2 and maternal age-dependent sister chromatid pre-division. However, even if not all the patients classified as TR/GC (M1) group have upd(15)mat due to conventional non-disjunction at M1, it can be concluded that maternal age-dependent factors still have a critical role in the occurrence of upd(15)mat in patients classified as TR/GC (M1) group. In addition, possible mixture of maternal age-dependent and -independent factors in patients classified as TR/GC (M2) group may be relevant to the lack of significant difference in the maternal age between TR/GC (M2) and Deletion groups, and between TR/GC (M2) and TR/GC (M1) groups.

Lastly, whereas fluorescence *in situ* hybridization analysis has been routinely performed at commercial laboratories since the year 1993 in Japan, detailed molecular studies including microsatellite analysis are usually available only in institutional laboratories. Thus, a substantial fraction of patients without deletions may have remained undiagnosed or misdiagnosed, without receiving further studies including micro-